Assessment of Microchannel Emulsification Technology using Different Materials

May 2015

Yanru ZHANG

Assessment of Microchannel Emulsification Technology using Different Materials

A Dissertation Submitted to
the Graduate School of Life and Environmental Sciences,
the University of Tsukuba
in Partial Fulfillment of the Requirements
for the Degree of Doctor of Philosophy in Bioresource Engineering
(Doctoral Program in Appropriate Technology and Sciences for
Sustainable Development)

Yanru ZHANG

TABLE OF CONTENTS

Nomenclature

CV	coefficient of variation [-]
d_{drop}	droplet diameter [m]
$d_{\text{n,drop}}$	number-weighted mean droplet diameter [m]
g	acceleration due to gravity [m/s^2]
Δh_{d}	height of a dispersed-phase chamber [m]
ΔP_{d}	pressure applied to a dispersed phase [Pa]

Greek symbols

θ	equilibrium contact angle [deg]
θ_{w}	water contact angle on MC plate [deg]
θ_{d}	contact angle of a dispersed phase [deg]
γ_{S}	solid surface free energy [J/m^2]
γ_{L}	liquid surface free energy [J/m^2]
γ_{SL}	liquid/ solid interfacial free energy [J/m^2]
ζ	zeta potential of MC plate surface [V]
σ	standard deviation [m]

Chapter 1

Introduction

1.1Emulsions

1.1.1 Definition

Emulsions have been utilized in various industries, including food, cosmetics, pharmaceutical, and chemical industries. An emulsion consists of two immiscible liquids, which one of the liquids dispersed as spherical droplets in the other. Emulsions droplets usually have an average diameter in the range of 0.1 to 100 μm. Emulsions can be conveniently classified according to the distribution of the oil and aqueous phases. A system, which consists of oil droplets dispersed in an aqueous phase, is called an oil-in-water (O/W) emulsion shown in Figure1-1a. Figure 1-1b shows a system which consists of water droplets dispersed in an oil phase is called water-in-oil (W/O) emulsion. Emulsions play an important role in the formulation of some O/W food emulsions, e.g., dressings, artificial milk, margarines and low fat spreads. Some emulsions are end products in themselves, e.g., coffee creamers and cream liqueurs are relatively simple emulsions which remain stable towards creaming and coalescence during their production and shelf-life. Emulsions can also be used as ingredients, which participate in forming the structures of more complex products. For example, yoghourts and their gelled system contain emulsion droplets that must interact with other food ingredient, but that must not be destabilized in the process. Finally, the emulsion droplets may create new structures, i.e., in ice cream or whipped products, where the emulsion itself is required to destabilize as a means to creating structure in the product. The substance that makes up the droplets in an emulsion is called the dispersed or internal phase, whereas the substance that makes up the surrounding liquid is referred to as the continuous phase of external phase.

It is possible to form an emulsion by homogenizing pure oil and pure water together,
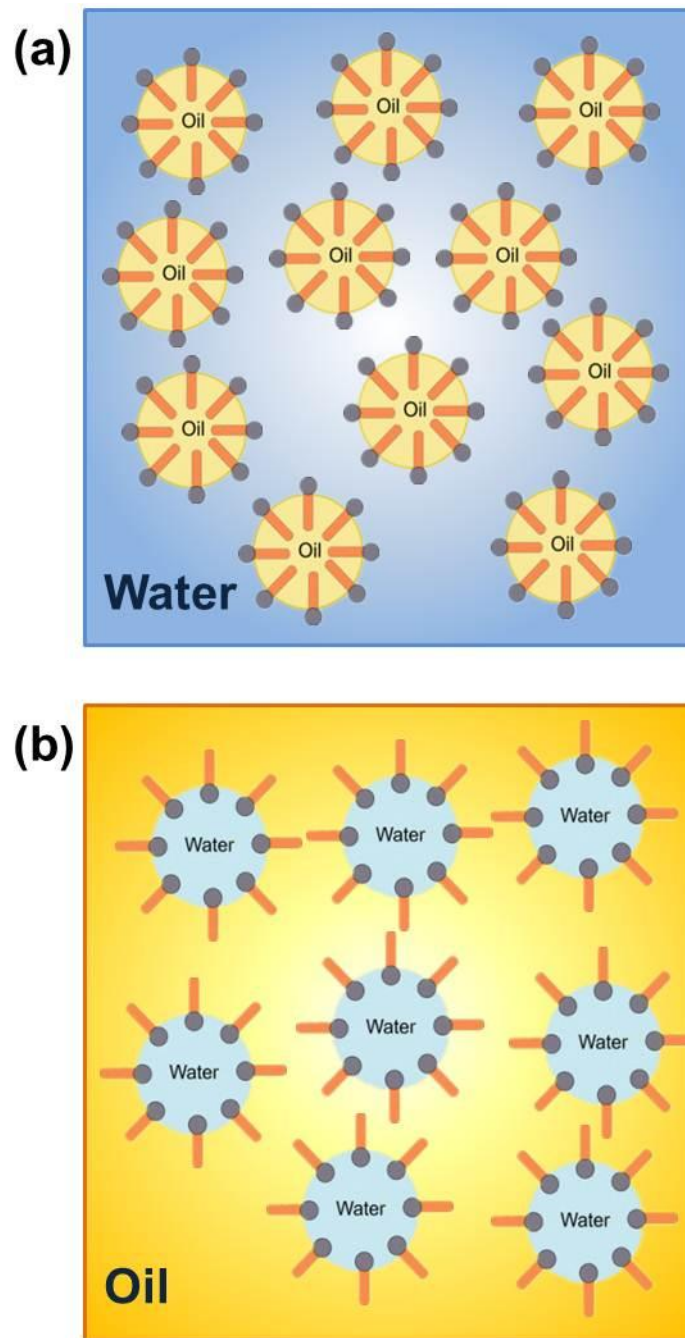
Figure 1-1 Schematics drawing of emulsion types. (a) an oil-in-water (O/W) emulsion. (b) a water-in-oil (W/O) emulsion.

but the two phases usually rapidly separate into a system that consists of a layer of oil (low density) on top of a layer of water (high density). This is because droplets tend to merge with their neighbors when they collide with them, which leads to complete phase separation. The driving force for this to happen is that the contact between oil and water molecules is thermodynamically unfavorable (Israelachvili, 1992); emulsions are thermodynamically unstable systems. It is possible to form emulsions that are kinetically stable for a reasonable period of time, by including substance known as stabilizers. The stabilizer enhances the stability of an emulsion and may be classified as either an emulsifier or a texture modifier depending on its mode of action. Most emulsion formation by diminishing interfacial tension and stabilizes the formed emulsions by inducing a repulsive force between droplets (Dicknson, 1992). Emulsions are surface active molecules that absorb to the surface of freshly formed droplet during homogenization, forming a protective membrane that prevents the droplets from coming close enough together to aggregate.

1.1.2 Droplets size and size distribution

Many of the most important properties of emulsion-based food products are determined by the size of the droplets that they contain, e.g., shelf life, appearance, texture, and flavor. Consequently, it is important to be able to control, measure, predict and report the size of the droplets. The droplet size affects the taste and appearance of a product. For example, an O/W emulsion with smaller droplets suppresses bitterness (Nakaya *et al*., 2006). And emulsion with larger droplets will be more opaque and whitish, white emulsions with smaller droplets will be more transparent. The droplet size distribution affects many of the physicochemical properties of the emulsion. In

addition, because W/O food products (e.g., margarine) contain flavoring components in the dispersed phase, the droplet size distribution affects the flavor of such a product. Droplet size distribution may also have a great effect on growth bacteria. When the droplets diameter is large, bacteria multiply more easily than for smaller droplet diameter, as the bacterial growth is reduced due to the lack of nutrients inside the droplets. The stability of the emulsion in terms of emulsion susceptibility against destabilization into two or more separate phases is influenced in different ways. It is important to have information about the full droplet size distribution of an emulsion. However, knowledge of the most useful numbers, which are the average droplet size of emulsion and the width of the distribution, is sufficient in many situations (Hunter, 1986). The average diameter is a measure of the central tendency of the distribution, and the standard variation is a measure of the distribution. The coefficient of variation, defined as one hundred times the standard deviation divided by average diameter, is a measure of the distribution relative to the average diameter.

1.1.3 Monodisperse emulsions

The stability of emulsions is an important factor for various industrial branches, such as the food, pharmaceutical and cosmetics industries. Monodisperse emulsions are helpful in controlling the stability and in studying the fundamental mechanisms that lead to their instability (Mason *et al.,* 1996a). Generally, there are two fundamental mechanisms that lead to instability in emulsions. One is an Ostwald ripening; this entails the molecular diffusion of the liquid in the dispersed phase through the continuous phase, allowing transfer from one droplet to another (Taylor, 1998). The other one which causes instability is coalescence, by cloud droplets collide, then join

together to form a larger droplet.

Monodisperse emulsions are useful for fundamental studies because the interpretation of experimental results is much simpler than that for polydisperse emulsions (McClements, 1999). For example, the stability of droplets can be monitored very simply, since changes in the droplet size are easily studied by having monodisperse droplets.

The better stability and simplified physicochemical properties of monodispersed emulsions are also applicable to various industrial fields that produce valuable emulsion-based products, such as functional microparticles, and microcapsules and multiple emulsions.

It is clear that the droplet size and droplet size distribution are both important for the properties and stability of emulsion based products. However, traditional techniques to produce emulsions are far from optimal to fulfill the requirements for desired emulsion properties, but a number of new techniques have the potential to do so. We will therefore first discuss some of the traditional emulsification techniques, and subsequently some of the newer techniques.

1.2 Emulsification devices

1.2.1 Conventional emulsification

Usually, emulsions are produced starting from a coarse pre-mix emulsion obtained by gentle mixing, followed by using homogenization to further reduce the droplet size. In general, homogenization is an intense process: it introduces large amount energy into the premix emulsion to break up the droplets into smaller ones. The actual emulsification is performed by disrupting the pre-mix droplets in intense laminar or

turbulent flow, or a combination of those, where the shear forces on the droplets have to exceed the interfacial tension forces that keep a droplet together for droplet break up. In order to facilitate the creation of an emulsion with small droplet sizes, lowering the interfacial tension by adding an emulsifier is advantageous. It should be kept in mind that not only the interfacial tension itself but also the rate at which emulsifiers adsorb to the interface is of importance. A high adsorption rate causes a newly formed droplet to quickly lower its interfacial tension, possibly leading to further disruption. Additionally, re-coalescence is prevented by quickly stabilizing the formed droplets.

Major homogenization systems that are used in practice are:

High pressure systems (Figure 1-2a), in which the premix emulsion is pushed through a small orifice at high pressure. Due to the high shear and extension rates in the orifice, the droplets break up into smaller droplets.

Rotor-stator systems (Figure 1-2b), in which the premix emulsion is pushed through the gap between a cylindrical or conical stator and rotor. Due to the shear and extension exerted by the rotor the droplets break up into smaller droplets.

Ultrasound systems (Figure 1-2c), in which the premix is placed in a vessel with an ultra sound device. Due to the intense turbulence caused by the ultrasound waves, the droplets break up into smaller droplets.

In all of these systems the energy input is orders of magnitude higher than necessary for the formation of the extra interfacial area. This results in damage of possible fragile components in the product, and often in a significant increase in temperature. These process can be classified as being energy inefficient (McClements, 2004), about 90-99% of all energy is not used in droplet breakup. Another disadvantage of these methods is the relatively wide droplet size distribution they yield (Saito *et al.*,
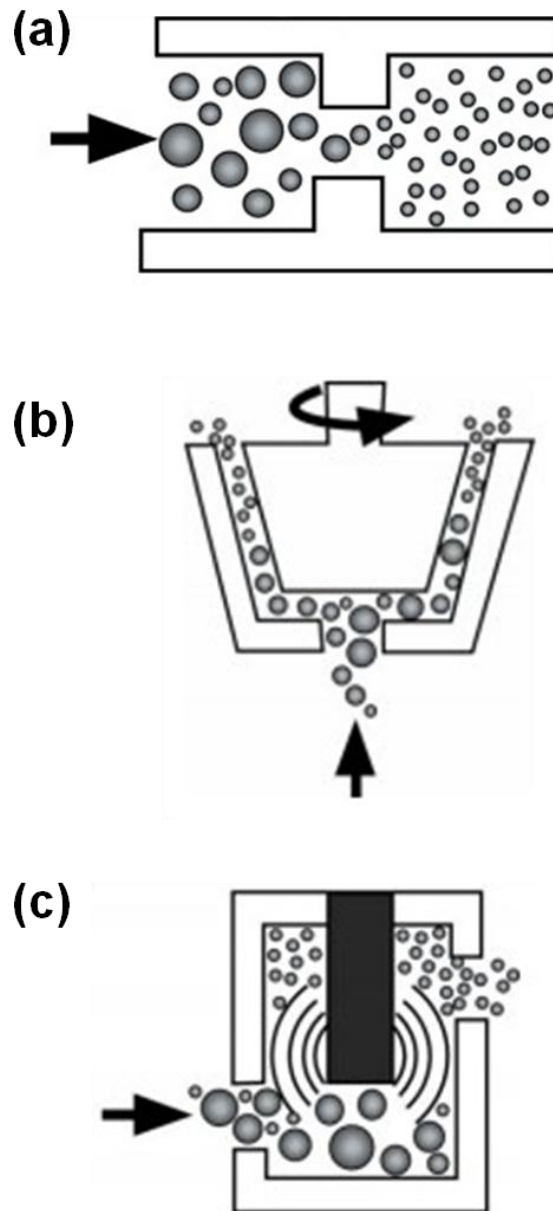
7

Figure 1-2 Schematic representation of traditional emulsification apparatuses. (a) high pressure homogenizer, (b) rotor-stator homogenizer, (c) ultrasound homogenizer.

2006). There have been many efforts to optimize the methods with respect to energy input and droplet size distribution, but the actual amount of energy that is used is much larger than would be theoretically necessary, and the droplet size distributions of the emulsions are still far from monodisperse.

1.2.2 Emulsification with membranes and microfluidic devices

Recently, new methods for emulsification, which use microfluidic devices, have received much attention in literature. Membrane emulsification is one of them which attracted increasing attention to food, pharmaceutical, chemical, and cosmetic industries over the last two decades.

Membrane emulsification, in which the pressurized dispersed phase passes through a microporous membrane and forms emulsion droplets (Figure 1-3), is a promising technique for producing and forms monodisperse emulsions with a coefficient of variation of approximately 10% (Nakashima *et al.,* 1991; Suzuki, 1994). This technique is applicable to both O/W emulsions using hydrophilic membranes and W/O emulsions using hydrophobic membranes (Suzuki, *et al.,* 1996; 1998). The emulsions are produced by pressurizing a dispersed phase into a continuous phase, and the emulsion droplet size is controlled by the membrane pore size. This technique can be used to produce emulsions without strong mechanical stress (Schröder *et al.,* 1997). Furthermore membrane emulsification processes allow the production of emulsions at lower energy input (10^4-10^6 J/m^3) compared with conventional mechanical methods (10^6-10^8 J/m^3). Recently, the insights into the droplet formation mechanism were proposed (Schröder *et al.,* 1998; Peng and Williams, 1998). In their models, the droplet size is determined by the cross-flow velocity of the continuous phase, the pore diameter, the trans membrane
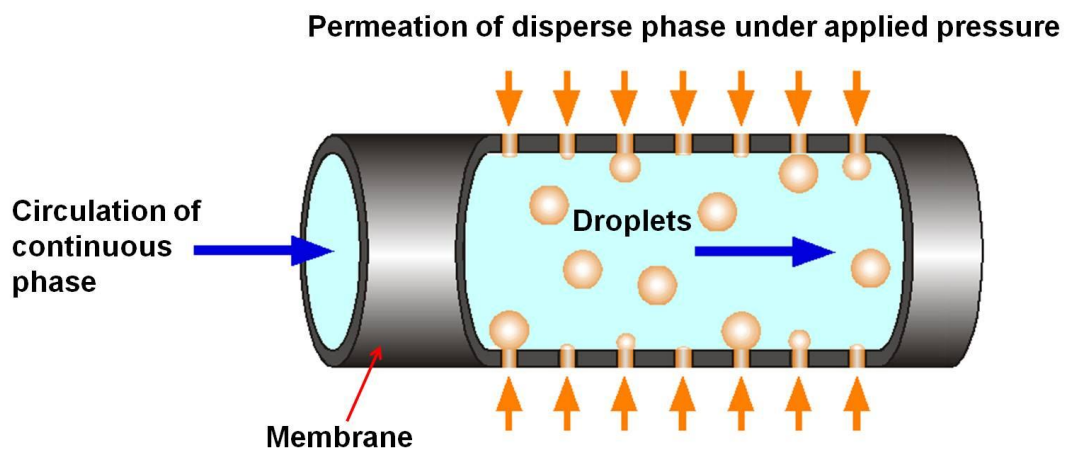
9

Permeation of disperse phase under applied pressure

Circulation of continuous phase

Droplets

Membrane

Figure 1-3 Schematic diagram of the membrane emulsification process.

pressure, and the (dynamic) interfacial tension. Using this model, the droplet formation process was calculated by computational fluid dynamics (Abrahamse *et al.,* 2001). Abrahamse *et al.,* (2004) microscopically visualized droplet formation via a micro-engineered membrane with uniform pores. Although the membrane pores were uniform in size, the prepared emulsions were polydisperse. They also demonstrated that this result is due to steric hindrance of droplets forming simultaneously. Kobayashi *et al.,* (2002) performed a real-time microscopic observation of emulsion droplet formation from a polycarbonate membrane. They investigated the effect of the crossflow velocity of a continuous phase and the surfactant type on droplet size.

This direct droplet formation method with membranes and the rapid development in microtechnological engineering in the electronics technology led to devices in which droplet formation could be achieved in channels in the same size range as the droplets themselves. Microfluidic devices distinguish from traditional membranes by their precisely designed geometry of pores and channels, which makes them suited for the production of small and monodisperse droplets (Kobayashi and Nakajima, 2006).

1.2.3 Microfluidic channels for emulsification

Microfluidic channels consist of grooves and through-holes with a size of 1 to 1000 μm microfabricated on a chip. One can carry out various kinds of liquid operations in the well-designed microfluidic channels, exploiting a micrometer-sized space. Rapid advance in microfabrication technology enables precise fabrication of networks and arrays of the microfluidic channels. For most emulsification technologies using microfluidic devices, the dispersed phase that passed through the channel is directly broken up into droplets. This droplet-generation process suggests that the resultant

11

droplet size and its distribution greatly depend on the channel size and its distribution. Thus, the microfluidic channels precisely controlled in size and its distribution are useful for generation of monodisperse emulsion droplets with a desired size.

1.2.4 Channel materials and their surface properties

Microfluidic channels for emulsification are generally made of silicon, silicon compounds, polymers, and metal (Table 1-1). Their typical fabrication techniques, listed in Table 1-1, include chemical wet etching, chemical dry etching, mechanical cutting, injection molding, soft lithography, and electroforming, being described in detail in Nguyen *et al.,* 2002. The etching techniques enable precise fabrication of the microfulidic channels with a size of over 1μm. It is also possible to fabricate submicrometer channels by these techniques. The channels precisely fabricated by the other fabrication techniques have typical size greater than 10 μm. The inherent surface affinity of the channel materials, such as hydrophilic and hydrophobic, plays an important role in the emulsification behavior. Hydrophilic channel materials include surface-oxidized silicon, silicon compounds and stainless steel. Hydrophobic materials include polymers and nickel. Preventing the dispersed phase from wetting on the channel surface is a prerequisite for generation of monodiserse emulsion droplets from the channel. The most significant strategy for the successful droplet generation is to select the dispersed phase liquid with a surface affinity different from that of the channel. Therefore, hydrophilic and hydrophobic channels are commonly used to generate O/W and W/O emulsion droplets, respectively. The surface charge of the channel materials is also a key factor affecting the emulsification behavior.

Table 1-1 Materials of microfluidic channels for emulsification

Materials	Fabrication techniques	Inherent surface affinity	Ref.
Surface-oxidized silicon	Anisotropic wet etching Chemical dry etching	Hydrophilic	Kawakatsu *et al.,* (2004) Xu *et al.,* (2004) Kobayashi *et al.,* (2002)
Quartz glass cutting	Mechanical	Hydrophilic	Nishisako *et al.,* (2004)
Pyrex grass etching	Isotropic wet	Hydrophilic	Okushima *et al.,* (2004)
Photostructurable glass	Chemical dry etching	Hydrophilic	Herweck *et al.,* (2001)
Silicon nitride	Chemical dry etching	Hydrophilic	Van der Graaf *et al.,* (2004)
Poly (dimethylsiloxane) (PDMS)	Soft lithography	Hydrophilic	Anna *et al.,* (2003); Link *et al.,* (2004); Zheng *et al.,* (2003)
Poly (methylmethacrilate) (PMMA)	Mechanical cutting	Hydrophobic	Nishisako *et al.,* (2002)
	Injection molding	Hydrophobic	Liu *et al.,* (2004)
Urethane	Soft lithography	Hydrophobic	Thorsen *et al.,* (2001)
Stainless steel	Mechanical cutting	Hydrophilic	Tong *et al.,* (2001)
Nickel process	LIGA[a]	Hydrophobic	Gu *et al.,* (2000)

a) LIGA: Lithographie, Galvanoformung, Abformung.

For example, the surface-oxidized silicon, which is in contact with the continuous water phase, has a negative surface charge (Gu *et al.,* 2000). Tong *et al.,* (2001) reported the effect of the surfactant charge on the emulsification behavior using a silicon array of the channels. The use of anionic surfactants, which have a repulsive interaction with the negatively charged channel surface, led to successful generation of monodisperse O/W emulsion droplets from the channels. In contrast, the use of cationic surfactants, which have an attractive interaction with the negatively charged channel surface, resulted in generation of polydisperse emulsions droplets from the channels and wetting of the dispersed phase on the channel surface. We thus have to select an appropriate

combination of the channel material, the two liquid phases, and the surfactant to achieve successful generation of monodisperse emulsion droplets using the microfluidic channels.

1.2.5 Microchannel emulsification

Kikuchi *et al.* (1992; 1994) developed a system in which a microscope was attached to a video recorder (microscope video system) for viewing optically accessible uniform microchannels (MCs) formed in a single crystal silicon substrate, which was manufactured with semiconductor technology. Kawakatsu *et al.* (1997) proposed MC emulsification to form monodisperse emulsion droplets using MC arrays, fabricated on a single-crystal silicon microplate. The silicon plate including MC arrays was originally developed as a capillary vessel model for blood rheology measurements and analysis (Kikuchi *et al.,* 1992; 1994). MC emulsification enables producing uniform droplets with a small coeffient of variation of bellow 5%. The droplet generation unit used in MC is a microchannel array consisting of parallel MCs with a terrace and a deep well (Figure 1-4). Droplets are directly generated in the well via an MC array, even in the absence of a cross-flowing continuous phase. This droplet generation based on spontaneous transformation is very mild process and has very high energy efficiency (Sugiura *et al.,* 2001). MC emulsification plates consisting of grooved MC arrays (Figure1-4a) have very low productivity of oil droplets (<0.001 m^3/ (m^{2}h) for vegetable oil) when MCs with a characteristic size of 10 μm are used. A straight-through MC array consisting of highly integrated microfabricated through-holes (Figure 1-4b) remarkably improved the droplet productivity of MC emulsification (Kobayashi *et al.,* 2002). Straight-through MC arrays with an MC size of 10 μm produced monodisperse

vegetable oil droplets at a maximum dispersed-phase flux of 0.06 m^3/ (m^{2}h) (Kobayashi *et al.,* 2003). MC emulsification is capable of producing monodisperse emulsions with droplet sizes of 1μm to 200 μm using grooved MC arrays (Kawakatsu *et al.* 1997; Kobayashi *et al.,* 2007) or straight-through MC arrays (Kobayashi *et al.,* 2005; 2010). Droplet generation for MC emulsification is driven by the difference in Laplace pressure acting on the oil-water interface in the well and on the terrace (Sugiura *et al.,* 2001). This droplet generation is not basically influenced by the flow rate of the continuous phase (Kobayashi *et al.,* 2002). The size and uniformity of the resultant droplets are also independent of the flow rate of the dispersed phase through the channels below a critical value (Sugiura *et al.,* 2002a; Kobayashi *et al.,* 2003). These robust features are appropriate for practical production of monodisperse emulsions.

1.3 Surface property of silicon MC plates

1.3.1 Contact angle and Young equation

The angle formed by the solid surface and the tangent line to the upper surface at the end point is called the contact angle**.** The contact angle is a result of the interface/surface tensions (surface free energies) between liquid and solid surrounded by vapor, and is measured according to the Young equation:

$$\gamma_s = \gamma_L \cdot \cos \theta + \gamma_{SL} \tag{1-1}$$

where γ_s is the solid surface free energy, γ_L is the liquid surface free energy, γ_{SL} is the liquid/ solid interfacial free energy, θ is the equilibrium contact angle. The Young's equation assumed a perfectly flat surface, and in many cases surface roughness and impurities cause a deviation in the equilibrium contact angle from the contact angle predicted by Young's equation.

1.3.2 Typical contact angle

If the molecules of a liquid are strongly attracted to the molecules of a solid (for example water on a strongly hydrophilic solid) then a drop of the liquid will completely spread out on the solid surface, corresponding to a contact angle of 0°. Weaker attractions between liquid and solid molecules will result in higher contact angles. On many highly hydrophilic surfaces, water droplets will exhibit contact angles of 0° to 30° (Figure 1-5a). If the solid surface is hydrophobic, the water contact angle will be larger than 90° (Figure 1-5b). Highly hydrophobic surfaces made of low surface energy (e.g. fluorinated) materials may have water contact angles as high as ~120°. Some materials with highly rough surfaces may have a water contact angle even greater than 150°, due to the presence of air pockets under the liquid drop. These are called superhydrophobic surfaces. Sometimes the contact angle is measured through the gas instead of through the liquid, which would replace all of the mentioned angles by 180° minus their given value. Solid materials like metals and glasses generally have large surface free energy (the γ_s should be large) and water droplets on those materials should form a small contact angle. On the other hand, when the solid surface is contaminated with organic materials, water droplet will form a larger contact angle. The contact angle is sensitive enough to show different results even with a small amount of contamination such as monolayer orders. Thus, contact angle can be used for evaluating cleanness and hydrophilicity of solid surface.
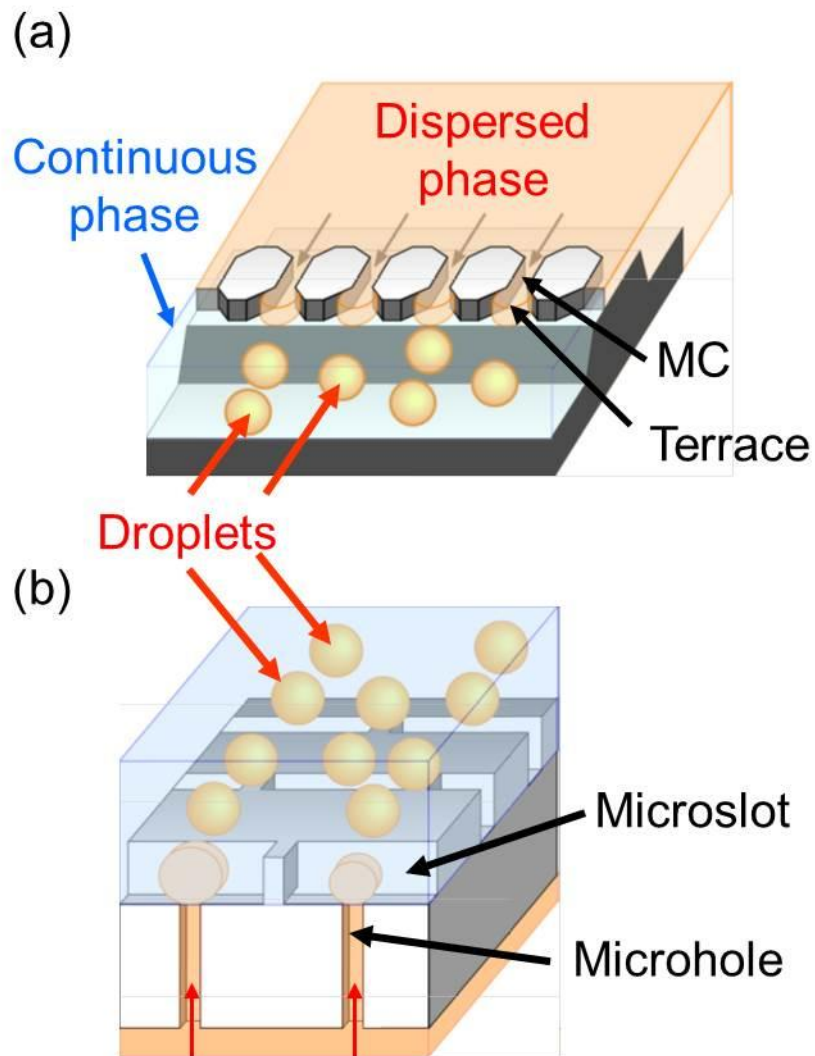
Figure 1-4 Schematic drawings of droplet generation via part of grooved MC array (a) and part of an asymmetric straight-though MC array (b); (Kobayashi and Nakajima, 2004).
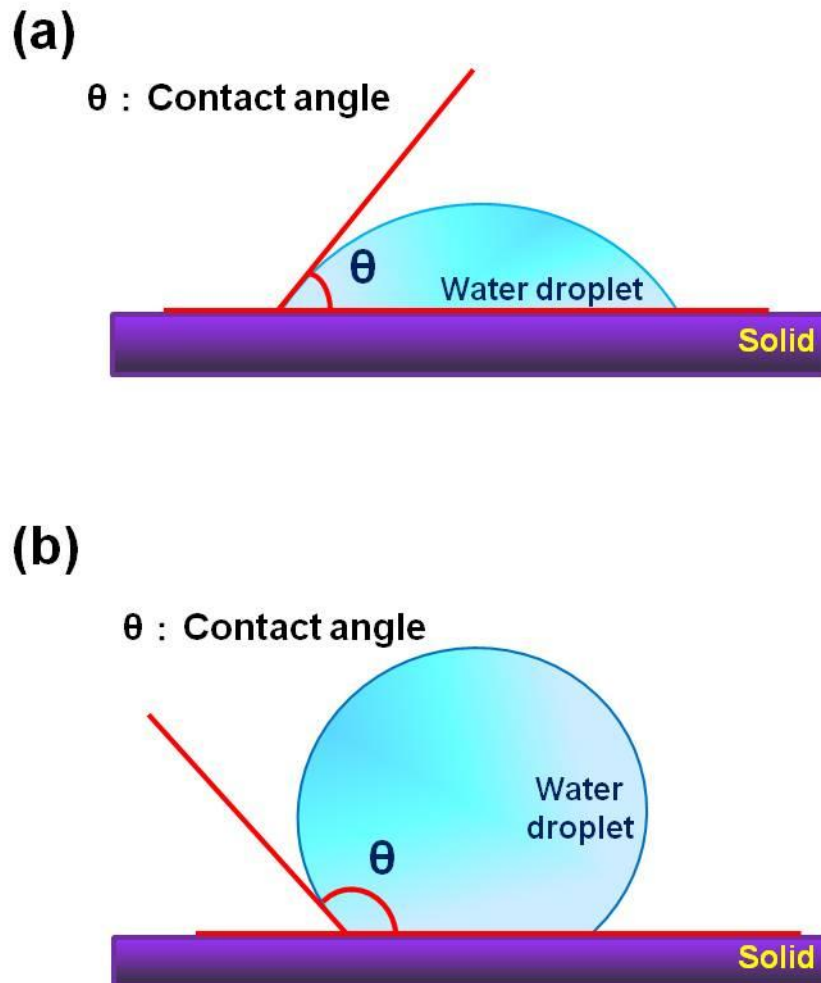
Figure 1-5 Schematic drawing of the typical water contact angle to the solid surface. (a) Hydrophilic solid surface with a contact angle lower than 90°. (b) Hydrophobic solid surface with a contact angle larger than 90°.

1.3.3 Contact angle measurement method

The $\theta/2$ method (a half angle method) is generally used to determine the contact angle. The method calculates the contact angle from the angle (θ_1) between the droplet base line and the line passing beyond the apex of the droplet as shown in the Figure1-6. Based on the assumption that the droplet profile forms a segment of an arc, $2\theta_1=\theta$ is formulated by geometric theorem. The $\theta/2$ method essentially supposes that the droplet forms a partial sphere. Therefore, if the droplet becomes non-spherical due to gravity, an inaccurate measurement will result.

1.3.4 Surface property of silicon MC plates

In MC emulsification, single-crystal silicon MC plates are normally used to produce monodisperse emulsions. The surface of MC plates must remain sufficiently hydrophilic during production of O/W emulsions by MC emulsification. Prior to the first usage, MC plate are subjected to plasma oxidation in order to grow a hydrophilic silicon dioxide layer on the surface of the MC plate (Kobayashi *et al.,* 2003) However, although the silicon MC plate was anisotropic wet etching period shipping but after stored for more than one year the water contact angle extremely increased and lost its hydrophilicity. Moreover it was difficulty in stably producing monodisperse emulsions for continuous emulsification. One emulsification experiment used butter as the dispersed phase indicated that stably produce monodisperse droplets were difficult to carry out after 24h continuous MC emulsification. Thus to stably produce monodisperse O/W emulsions, the hydrophilic plate surfaces must be kept during emulsification.

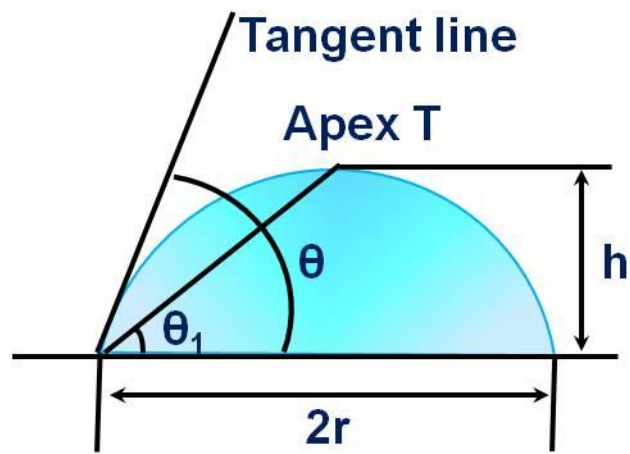### 1.3.5 Practical-scale production of monodisperse emulsions

Figure 1-6 Schematic drawing of θ/2 contact angle measurement method.

Uniform droplets generated by microfluidic techniques are useful templates for producing uniform microspheres and microcapsules (Sugiura et al. 2001b; Nakagawa et al.2004; Utada et al. 2005; Li et al. 2008). However, microfluidic chips usually have a very low throughput in terms of the volume flow rate of the dispersed phase (Q_d), since droplets are usually generated from one pair of short MC arrays for MCE or a single MC for the other microfluidic techniques. For instance, uniform fine (10 μm) droplets of triglyceride oil are generated using a current microfluidic chip at Q_d of $<10^{-2}$ ml h^{-1} ($<10^3$ droplets s^{-1}) for a flow-focusing geometry (Xu and Nakajima 2004) and of $<10^{-1}$ mL h^{-1} for an existing MC emulsification chip. This throughput would be difficult to satisfy even in laboratory-scale production. Thus, the scaling up of microfluidic emulsification systems is vital for increasing the number of MCs, although a few research groups have reported on mass production of droplets by microfluidic techniques over the last half decade (Kawai et al. 2003; Kobayashi et al. 2005; Nishisako and Torii 2008). Although the large microfluidic emulsification systems enabled mass production of uniform droplets with an average size of 30 μm (MCE) or 95 μm (cross-junctions), large microfluidic emulsification systems for uniform fine droplets have not yet reported. In principle, smaller cross junctions can be parallelized for producing uniform fine droplet. However, it is expected that it becomes difficult to precisely control the flows of the two phases and to prevent the clogging by small debris as the MC characteristic size decreases. In MCE, MCE chips consisting of microfabricated asymmetric through-holes (Kobayashi et al. 2005) are the most promising for mass-producing uniform droplets. The asymmetric through-holes must be miniaturized to produce fine droplets. However, it is not easy to precisely fabricate asymmetric through-holes with a cross-sectional size of <5 μm, even using cutting-edge

microfabrication technology. Even if MCE chips with the fine asymmetric through-holes were obtained, they would not be tolerable enough to handle during MCE.

Kobayashi et al., (2010) reported a MCE chip consisting of integrated MC arrays, fabricated by a commonly used etching technique. The MCE chip was capable of producing monodisperse emulsions with fine droplets of soybean oil with $d_{3,2}$ of 10 μm at a Q_d of 1.5 ml h^{-1}, achieving a sufficient throughput to mass produce uniform fine droplets at least on a laboratory scale.

Long-term continuous MC emulsification is another key factor for achieving practical-scale production of monodisperse emulsions. Tong *et al*. (2002) demonstrated a successful short-term production of a monodisperse oil-in-water (O/W) emulsion for up to 4 h. However, changes in droplet generation during long-term continuous MC emulsification have not yet been studied.

1.3.6 The material of MC emulsification chips

MC emulsification chips are normally made of silicon-based materials, which are superior in terms of precise machining of MC arrays with uniform-sized channels. However, silicon chips have few drawbacks, such as shock fragility and intolerance against alkali cleaning. Aluminum and stainless-steel are practically more suitable materials due to chemical-proof surfaces and superior mechanical strengths. The superior mechanical strength of these two materials is also suitable for handling and repeated use of these chips for longer period of time.

Tong et al., (2001) developed a grooved MC array consisting of only parallel channels on a stainless-steel chip capable of producing monodispersed droplets with

diameter ranging from 20 to 210 μm. The channels fabricated individually by microcutting lacked precisely uniform size, confirming the difficulty to obtain monodisperse emulsions using stainless-steel chips.

Recently, Kobayashi et al., (2008) developed a stainless-steel MC array consisting of precisely microfabricated parallel channels and a terrace. It had the potential of producing highly monodisperse O/W emulsions with droplets diameter ranging from 350 μm to 570 μm, and CV below 1% with several milliliters per hour scale of droplet productivity.

Kobayashi et al., (2010) also reported the mass production of uniformly sized droplets on a liter per hour scale using a large MC emulsification device, capable of producing uniform sized oil droplets with average diameter of 87 μm and CV below 2%. Application of MC emulsification in industrial production requires not only large scale MC device development, but also needs to consider the generic use of the MC array chips of various materials. The need for generic use of metallic MC arrays with mass production ability has been arising. Prior to developing large scale metallic MC arrays, the droplet generation characteristics of metallic asymmetric straight-through MC array chip should be investigated.

1.4 Objectives and constitution of the thesis

The structure of the thesis is shown in Figure 1-7. The thesis starts general introduction, which includes the overview of emulsion, emulsification method, surface properties of silicon MC plate and main issues related to MC emulsification (Chapter 1). The main part of the thesis is composed of three parts. The first part analyzed the effect of storage conditions on water contact angle to silicon MC plate (Chapter 2). In this

chapter we als analyzed the effect of surface properties of MC plate on droplet generation. We measured contact angles of dispersed phase to the channel wall. Using contact angle data obtained in Chapter 2 and droplets generation observation data to certify surface condition will influence the droplet generation in MC emulsification. We also analyzed the effect of continuous emulsification on droplets generation (Chapter 3) by integrating conclusions we got in Chapter 2. These two chapter had talk about assessment for stable and practical scale production of MC emulsification. In chapter 4, we developed an asymmetric metallic straight-through microchannel arrays and evaluation of its production characteristics. This is assessment for generic use of MC emulsification. In the final chapter we will make a comparison of MC emulsification device which fabricated with different material. And the thesis will closed by general discussion. Finally, the thesis is brought to conclusions (Chapter 5).

The goal of this research is clarify the optimum storage conditions of hydrophilically treated silicon MC plate and elucidate the conditions for stable continuous MC emulsification. We focus on storage medium, storage temperature, storage pH and storage time of MC plate, we evaluating the storage consequent by monitor the time course of the water contact angle on MC plate. This study also investigates the droplet size, droplet size distribution and droplet generation in continuous MC emulsification by using different emulsifiers. To elucidate the conditions of stable continuous MC emulsification which could achieve practical-scale production of monodisperse emulsions. Another objective is to obtain some useful information for the development of large scale metallic MC emulsification device which could achieve generic use of MC emulsification.

Outline of the thesis

Chapter 2: The aim of this study was to find out a suitable plate storage condition which can maintain the hydrophilicity of the surface treated MC plates for a long period of time. This study also investigated the zeta potential of the MC plate surface in different liquid. The effect of surface properties of MC plate on droplet generation was investigated. We focus on droplet size, droplet size distribution and droplet generation by using MC plates with different surface conditions by MC emulsification containing different emulsifiers. We also investigate the dynamic contact angle of dispersed phase to channel wall using two different emulsifiers.

Chapter 3: Droplet generation during continuous MC emulsification was investigated. We focus on droplet size, droplet size distribution and droplet generation by continuous MC emulsification containing different emulsifiers.

Chapter 4: In this chapter, we investigated the production characteristics of monodisperse oil-in-water (O/W) emulsions formulated by using newly designed asymmetric straight-through MC arrays made of aluminum.

Chapter 5: In this chapter, we made a comparison of droplet generation charteristics of different material of MC plate. From this chapter we hope that we could make a discussion of such materials applied on MC plate fabrication and give some useful information for people to chosen a suitable material for their MC emulsification experiment.

Chapter 6: This chapter summarizes the conclusions from the present subject and the research followed in the subject.
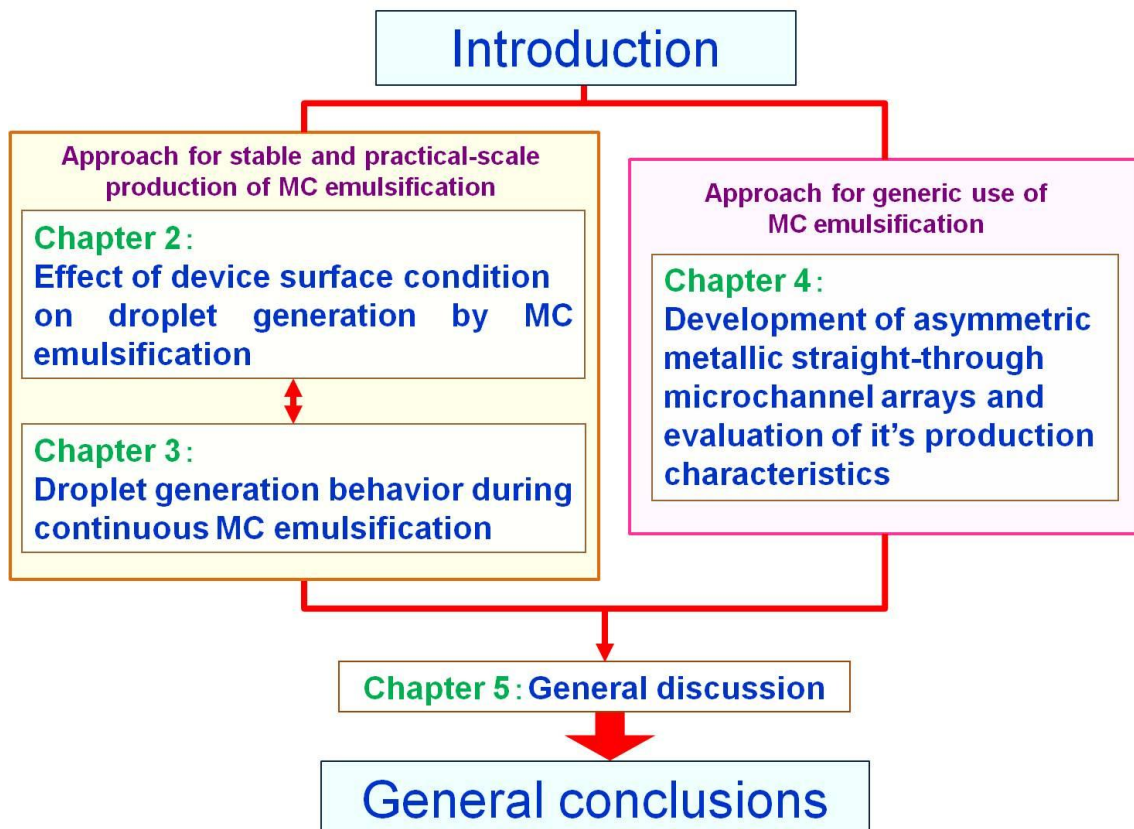
Figure 1-7 The general structure of this thesis.

Chapter 2

Effect of Microchannel (MC) Plate Storage Conditions on

Water Contact Angle

2.1 Introduction

Emulsions play an important role in various food products, such as mayonnaise, salad sauce, ice cream and so on. These food-grade emulsions are normally produced by conventional emulsification devices, e.g. high-pressure homogenizers and colloid mills, which apply intensive external forces to an emulsion system, usually produce polydisperse emulsions with empirically controlled average droplet diameters (McClements, 2004). Such external forces may cause damages to some bioactive components inside the resultant emulsions; their droplet size distribution may affect not only the taste but also the shelf life of the food product.

Recently, monodisperse emulsions consisting of uniformly sized droplets have received attention in various industries including food industry. Major advantages of monodisperse emulsions include simplified interpretation of experiment results, improved physical and qualitative stability, and the precise control of important emulsion properties (McClements, 2004). Monodisperse emulsions are also potential templates for producing various functional and advanced micro-materials which can further applied for preparing monodisperse microparticles, monodisperse microcapsules, and monodisperse giant vesicles (McClements, 2004; Mason et al., 1996).

Monodisperse emulsions could be prepared by several advanced emulsification techniques which use microstructured devices. Nakashima et al. (1999) proposed direct membrane emulsification that enables producing monodisperse emulsions with the smallest coefficient of variation (CV) of ~10% by permeating a dispersed phase through membrane pores into a continuous phase domain. This emulsification technique was previously used for industrial production of a low-fat spread, which is briefly introduced in a review (Nakashima et al. 2000) The cleaning process after membrane emulsification experiments is not straight forward and time consuming due to

three-dimensionally interconnected membrane pores. Microfluidic emulsification devices with different geometries, such as T-junction (Thorssen et al., 2001), cross-junction (Nisisako. et al., 2004) and Y-junction (Steegmans et al., 2009) can produce highly monodisperse single or multiple emulsions with droplet sizes larger than 10 μm on a chip. Glass capillary devices with a co-flow of two immiscible fluids are also capable of producing uniformed sized droplets (Utada et al., 2008). Dangla et al. (2012) presented a microfluidic device that utilizes height variations to generate monodisperse droplets. Li et al. (2014) demonstrated step-emulsification process using a microfluidic device with an abrupt (step-like) opening to a deep and wide reservoir, which could produce monodisperse emulsions. These microfluidic emulsification devices require the forced flow of two phases to successfully generate droplets. Successful membrane and microfluidic emulsifications are achieved when the surface properties of membranes and microfluidic channels are appropriately controlled (Vladisavljevic et al., 2013 and Shui et al., 2009).

Besides these microfabricated emulsification techniques, MC emulsification is also a promising and advanced technique for producing monodisperse emulsions with average droplet diameters of >1 μm and the smallest CV of <5% (Kobayashi et al., 2007, 2012). Droplet generation by MC emulsification is performed by simply forcing a dispersed phase through parallel microgrooves (grooved MC arrays) (Kawakatsu et al., 1997; Kobayashi et al., 2010) or deep micro-through-holes (straight-through MC arrays) (Kobayashi et al., 2005, 2010) into a (cross-flowing) continuous phase. Practical advantages of MC emulsification include the very mild droplet generation driven by interfacial tension dominant on a micron scale (Sugiura et al., 2001, Kobayashi et al., 2011) and the droplet size and its distribution insensitive to major operating parameters (Sugiura et al., 2002; Kobayashi et al., 2010, 2011).

Surface-treated silicon MC array plates are normally used for MC emulsification. These MC array plates are repeatedly used after cleaning and subsequent storage at room temperature. Hydrophilic MC array plates are usually stored in a hydrophilic liquid. However, their surface property tends to change during long-term storage, making it difficult to product monodisperse emulsions. Kobayashi et al. (2003) and Butron et al. (2011a) emphasized that an important point to successfully produce monodisperse oil-in-water (O/W) emulsions by MC emulsification is to avoid wetting of the dispersed phase to the plate surface. In other words, this successful MC emulsification can be achieved when using the MC array plates of appropriately high hydrophilicity. The contact angle between the dispersed phase and the plate surface in the presence of continuous phase is a useful indicator of predicting droplet generation behavior via MC arrays (Tong et al., 2000; Kobayashi et al., 2002a).

Due to the above reasons, hydrophilic treatment and storage conditions of MC array plates have to be appropriately controlled to successfully produce monodisperse O/W emulsions by MC emulsification. However, there is little information about the effect of the hydrophilic treatment and storage conditions of silicon MC array plates on the generation of O/W emulsion droplets via MC arrays. The primary aim of this study is to seek suitable storage conditions of silicon MC array plates that are hydrophilicity surface-treated. Another aim is to investigate how the surface properties of the silicon MC array plates stored in a fluid affect the generation characteristics of vegetable oil droplets from the rectangular channels. We also evaluated the surface properties of silicon MC array plates using the contact angle of a water drop on the plate and the contact angle of the dispersed phase to the MC wall in the presence of the continuous phase.

2.2   Materials and methods

2.2.1   Chemicals

Sodium azide, nitric acid, refined soybean oil, sodium dodecyl sulfate (SDS, hydrophilic lipophilic balance (HLB): 40), and polyoxyethylene (20) sorbitan monolaurate (Tween 20, HLB: 15) were purchased from Wako Pure Chemical Industries Ltd. (Osaka, Japan). The water used in this study was Milli-Q water with an electrical resistance of 18 MΩ cm.

2.2.2   Silicon MC array plate

Fig. 2-1 schematically illustrates the MC array plate (model MSX 11, Hitachi Haramachi Electronics Co., Ltd., Hitachi, Japan) used in this study. This $15 \times 15 \text{mm}^2$ plate made of single-crystal silicon was fabricated using a two-step photolithography and dry etching process (Kobayashi et al., 2002a). Four MC arrays with a length of 5 mm and a central through-hole with a diameter of 1 mm are formed on the front of this plate (Fig. 2-1a). Each MC array has 25 rectangular channels with a depth of 5 μm, a width of 20 μm, and a length of 2000 μm; the channels have a 20 μm-deep step at their inlets and outlets. As depicted in Fig. 1b, there is a flat surface on the back of the plate.

2.2.3   Effects of hydrophilic surface treatment and storage conditions of MC array plates

2.2.3.1 Hydrophilic surface treatment by plasma oxidation

The flat back of an MC plate was surface-treated with an oxygen plasma reactor (PR500, Yamato Scientific Co., Ltd., Tokyo, Japan) for 1 to 60 min at a chamber pressure of 15 Pa. Immediately afterwards, the hydrophilically treated plate surface was subjected to measurement of the static water contact angle defined in Fig. 2-2.
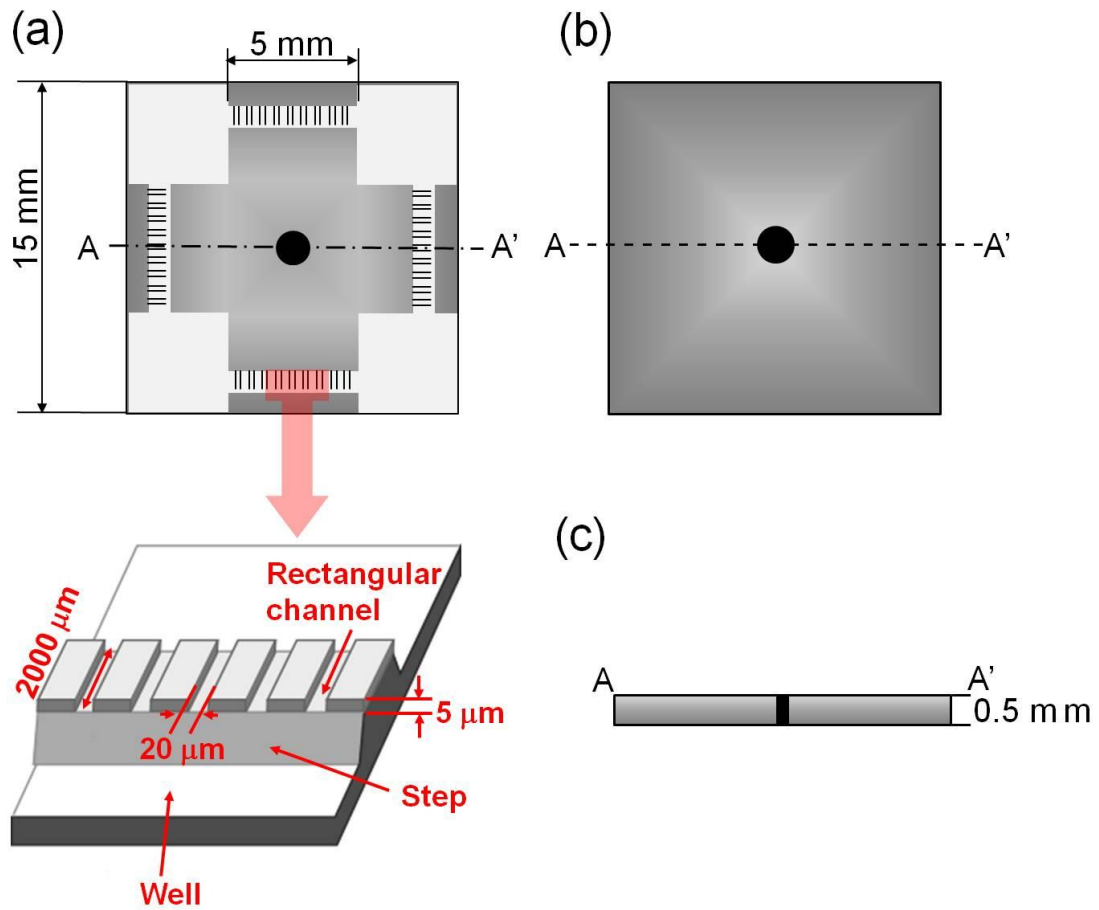
(a)

5 mm

15 mm

A ———————— A'

Rectangular channel

2000 μm

20 μm

5 μm

Step

Well

(b)

A ------------ A'

(c)

A ———————— A'

0.5 m m

Figure 2-1 Schematic representation of the silicon MC plate (model MSX). (a) Top view. (b) Three dimensional view of part of an MC array. (c) Back view. (d) Cross-sectional view.

33

2.2.3.2 Storage conditions of the surface-treated plates

After 15 min of the hydrophilic surface treatment, the MC array plates were stored in small glass vessels, each filled with air, nitric acid (10^{-5} to 10^{-1} mol/L) or Milli-Q water containing sodium azide (0.02 wt%) as antiseptic, for up to 10 to 30 days. Storage temperatures in each fluid were 5° C, 25° C, and 50° C.

2.2.3.3 Measurement of static water contact angle to the plate surface

Prior to contact angle measurement, the MC array plates stored in different fluids was rinsed with water, followed by their air-blow drying. We measured the static contact angles of 7 water drops to the flat surface of each MC array plate using the contact angle measurement mode of full automatic interfacial tensiometer (PD-W, Kyowa Interface Sciences Co., Ltd., Saitama, Japan). Each water drop with a volume of 0.5 μL was automatically dispensed from a needle attached to a syringe onto a selected position of the plate surface. The static water contact angles were determined from the captured images by θ/2 method, as depicted in Fig. 2-2.

2.2.4   MC emulsification

2.2.4.1 Setup and procedure

The MC emulsification setup used in this study consists of a module equipped with an MC array plate, a 10-mL liquid chamber containing the dispersed phase, a flexible tube with an inner diameter of 1 mm connecting the chamber and module, and a microscopic video system (Fig. 2-3) (Kobayashi et al., 2002a). During module assembly,
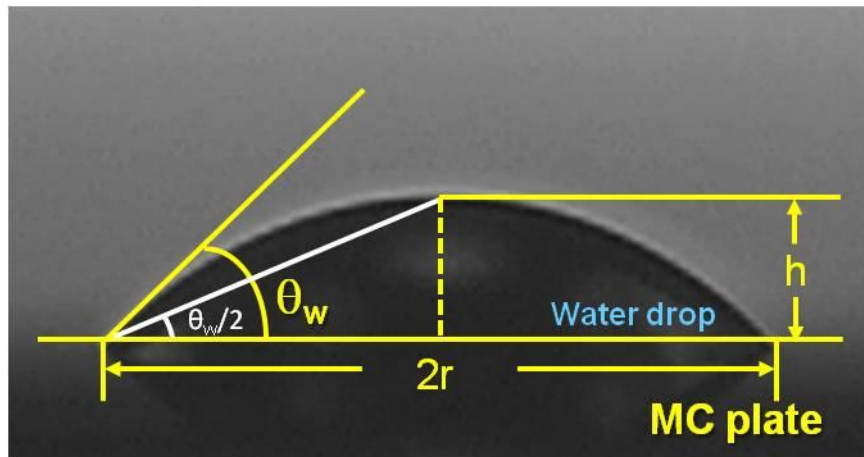
Figure 2-2 A captured image of a water drop onto the MC plate. θ is the static water contact angle to the plate surface.
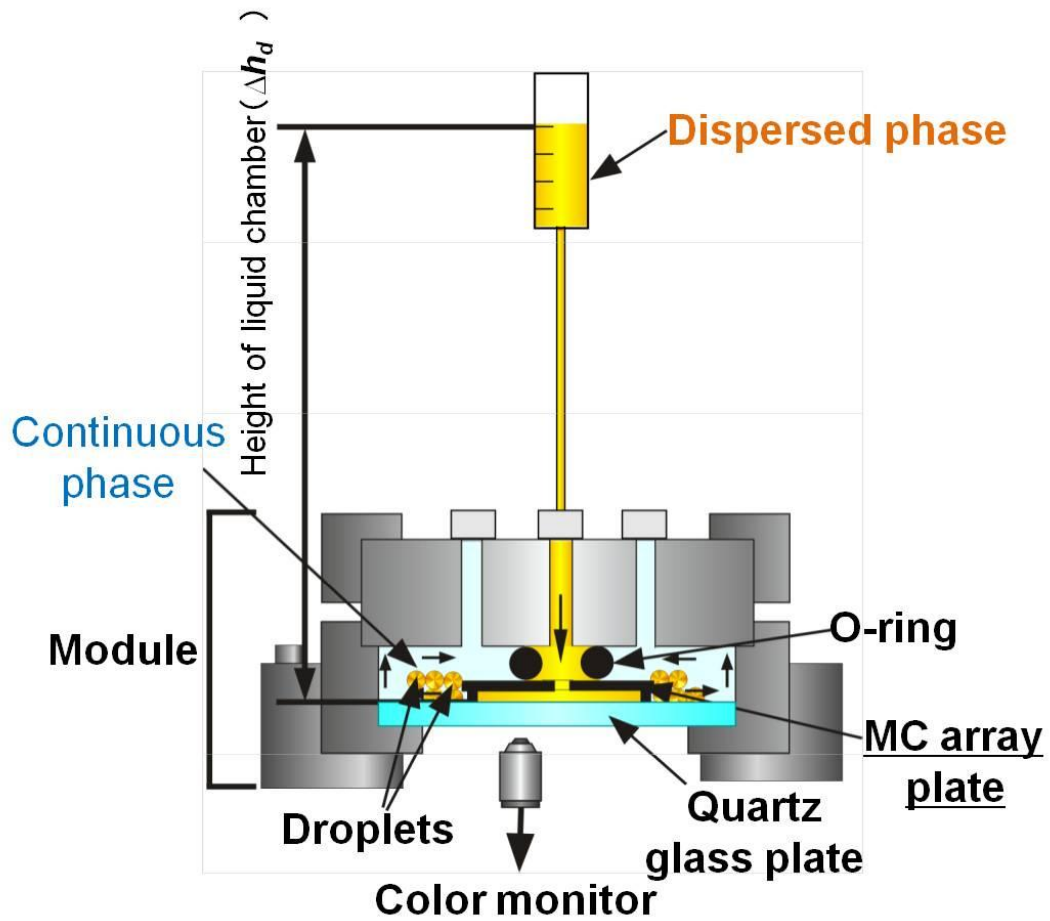
Figure 2-3 Simplified schematic drawing of the dynamic contact angle measurement setup which is also used as the MC emulsification setup.

the MC array plate was firmly attached onto a hydrophilic flat glass plate, and the compartments inside the module were filled with the continuous phase. The pressure applied to the dispersed phase (ΔP_d) in the module was determined by the following equation (Tong et al., 2000):

$$\Delta P_d = \rho_d \Delta h_d g \qquad (1)$$

where ρ_d is the dispersed-phase density (920 kg/m^3 for soybean oil), Δh_d is the difference in the hydraulic heads between the top of the dispersed phase in the liquid chamber and the MC array plate, and g is the acceleration due to gravity. Droplet generation was commenced by forcing the dispersed phase through the channels into the well filled with the continuous phase at a room temperature ($\sim 25^o$C). This droplet generation process was monitored in real time using the microscope video system.

2.2.4.2 Measurement of dynamic contact angle of dispersed phase to MC wall

The dynamic contact angle was determined based on the measurement method proposed by Butron Fujiu *et al.* (2011a). The dispersed phase was pressurized to enter the channels, and the oil-water interface was forced to very slowly advance in the channels (e.g. less than 10 μm/s). The dispersed phase moving forward inside a channel had a parabolic curve shape (Fig. 2-4a). The dynamic (advance/receding) contact angle to the MC wall was determined from images of an oil-water interface (Fig. 2-4b). Each contact angle was manually measured with a graphic editing program (Photoshop, Adobe Systems Incorporated, San Jose, USA) using the pen tool and direction handles. Afterwards, the dynamic contact angle (θ_d) was obtained by averaging the contact angle of 5 channels after calculated based on the following equation:

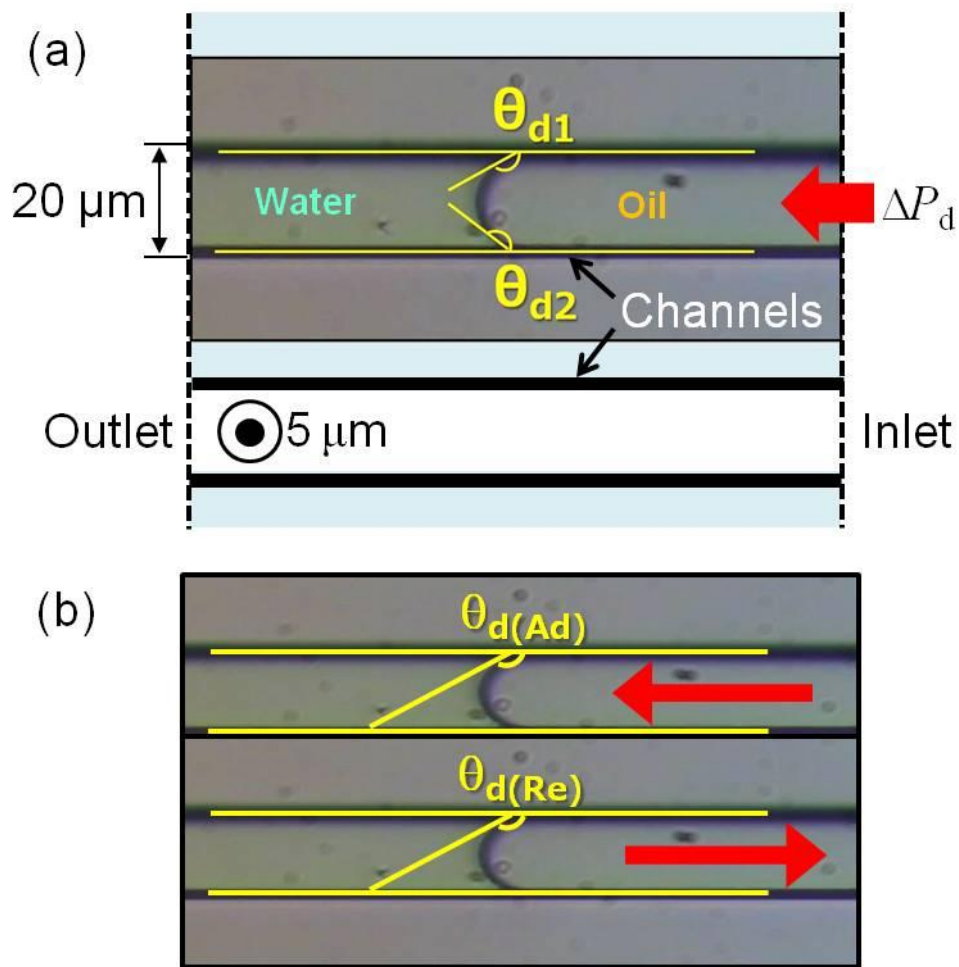$$\theta_d = \frac{\theta_{d1} + \theta_{d2}}{2} \qquad (2).$$

Figure 2-4 (a) Schematic of the contact angle measurement using parallel rectangular channels. θ_{d1} and θ_{d2} are the dispersed phase contact angles to the MC wall. (b) Schematic of the advancing and receding contact angles. $\theta_{d(Ad)}$ is the advancing contact angle measured when dispersed phase was advancing in the channels. $\theta_{d(Re)}$ is receding contact angle measured when dispersed phase was receding in the channels.

2.2.4.3 Droplet size analysis

The number-weighted mean droplet diameter ($d_{n,drop}$) was calculated using the diameter data of 100 droplets obtained from two different experiments. The diameter of each droplet was measured using image processing software (WinRoof ver.5.6, Mitani Co., Fukui, Japan). The droplet size distribution was expressed as a coefficient of variation (CV), defined as

$$CV = (\sigma/d_{n,drop}) \times 100 \qquad (3)$$

where σ is the standard deviation.

2.3 Results and discussion

2.3.1 Static water contact angle to silicon MC plate

2.3.1.1 Effect of surface oxidation time

Fig. 2-5 presents the water contact angle to the silicon MC plate before and after the surface treatment by oxygen plasma. The water contact angle to silicon MC plate surface was $84 \pm 4°$ before the surface treatment. However, the water contact angle decreased rapidly to $8 \pm 1°$ within 1 min of the surface treatment. The surface treatment time had negligible effect on the water contact angle to the MC plate. The image of water drop onto the MC plate after 15-min surface treatment is also shown in Fig. 2-5. This result demonstrates that the surface of MC plate was sufficiently hydrophilic. 1-min surface treatment led to greatly low water contact angle to the MC plate. To ensure a highly hydrophilic surface of the MC plate, we performed its surface treatment for 15 min in later sections.

2.3.1.2 Effect of storage conditions

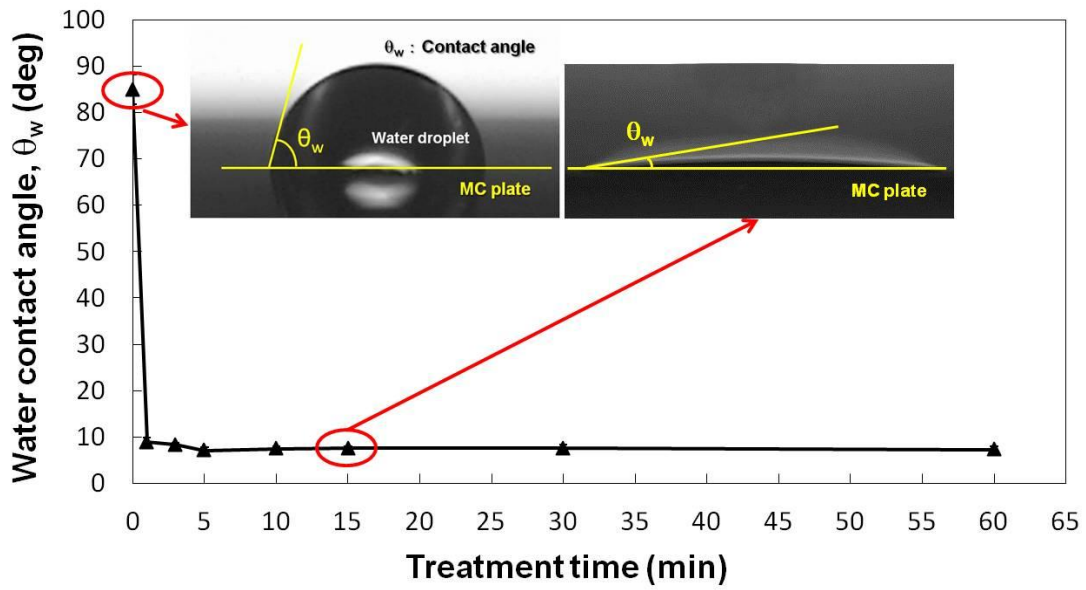Fig.2-6 shows the water contact angle data obtained using the MC plates stored in air

39

Figure 2-5 Effect of surface hydrophilic treatment time on water contact angle to silicon MC plate. The inset shows an image of a water drop on the MC plate surface-treated for 15 min. The water contact angle was 7.6°.

and nitric acid or Milli-Q water. For the plate storage in air, the contact angle values increased gradually with time, regardless of the temperatures applied. The rate at which the surface-treated MC plate surface loses its hydrophilic property was influenced by storage temperature. As can be seen in Fig. 2-6a, the increase of the water contact angle became remarkably faster at a storage temperature of $60^{o}C$ rather than at $5^{o}C$ and $25^{o}C$. Fig. 2-6b presents the water angle data obtained using the MC plates stored in 0.1 mol/L nitric acid. Similarly like the MC plates stored in air, the water contact angle increased gradually but more slowly with time for the MC plates stored in nitric acid, regardless of the temperatures applied. The water contact angles to the MC plate increased to $>30°$ after 10 days of storage. Their increasing rates were faster than those during storage in Milli-Q water. In contrast, the high hydrophilicity of the oxygen plasma treated MC plate surface was retained for extended periods of time when they were stored in Milli-Q water (Fig.2-6c). The increase in the measured water contact angles was found to be greatly smaller for the MC plates stored in Milli-Q water. The hydrophilicity of the MC plates stored in Milli-Q water was maintained well with small water contact angles of $20°$ to $25°$ after 10 days of storage. However, the water contact angle values increased gradually with time at $5^{o}C$ and $25^{o}C$. As can be seen in Fig. 2-6c, the water contact angle at day 30 increased to $>45°$ at $25^{o}C$ and $~35°$ at $4^{o}C$. Storage temperature somewhat affected the water contact angle after day 20.

It is presumed that the reason for different increasing rate of the water contact angle to the MC plates stored in these three medium can be explained by that air is a hydrophobic fluid, and it has a complex composition that composed of hydrogen, oxygen, carbon dioxide and water vapor. All of these may have some interaction with hydrophilic MC plate surface that make it lost its hydrophilicity. In addition, after stored in air at high temperature for long times, the hydrophilic silanol groups on the MC plate
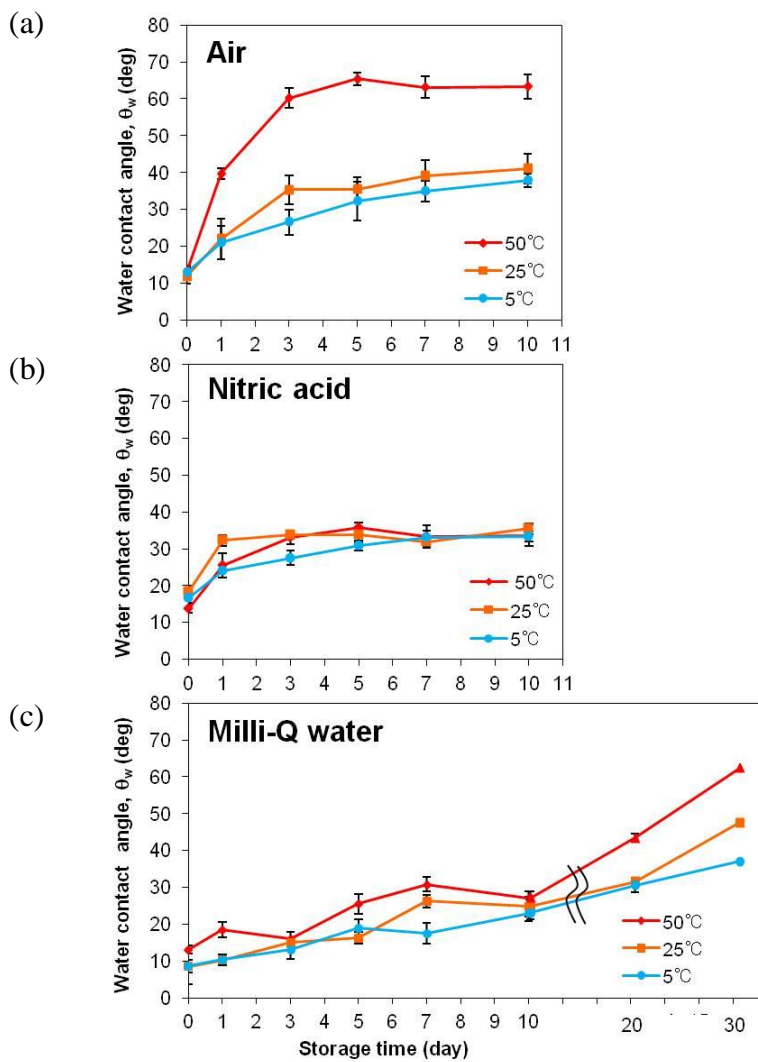
(a)

(b)

(c)

Figure 2-6 Time courses of water contact angle on the MC plates stored in air (a), nitric acid (b) and Milli-Q water (c) at different temperatures.

surface may escapes from the MC plate surface hydrophobic environment to the MC hydrophilic MC plate surface that make it lost its hydrophilicity. In addition, after stored in air at high temperature for long times, the hydrophilic silanol groups on the MC plate surface may escapes from the MC plate surface hydrophobic environment to the MC plate bulk. Also, the physical adsorption may take place into chemical adsorption and have an irreversible interaction on the MC plate surface when stored the plate at high temperature. However, although nitric acid is a hydrophilic fluid, nitric acid molecules were basically ionized into nitrate and hydrogen ions. The interaction between hydrogen ions and silanol group formed on the MC plate surface has a pronounced effect on the variation of its hydrophilicity. Milli-Q water is a hydrophilic fluid, and the concentration of dissociated hydrogen irons in the Milli-Q water is 10^6 times less than that in nitric acid. This may affect the difference in the variation of the hydrophilicity in terms of the water contact angle to the MC plate surface stored in nitric acid or Milli-Q water. This hypothesis can be supported by the value of MC plate surface zeta potential. The MC plate stored in water had a high negatively charged surface zeta potential about -200.41 mV (Fig. 2-7). In contrast, the surface zeta potential of MC plate stored in 0.1mol/L nitric acid was 0 mV which mean that most of negatively charged silanol groups on the MC plate surface were physically adsorbed with positively charged hydrogen irons. In contrast, the concentration of ionized hydrogen ion with positive charge in Milli-Q water is very small, making it difficult to interact with silanol group with negative charge formed on the MC plate surface. However while stored the MC plate more than 20 days, the temperature somewhat influence the hydrophilicity of plate surface. High-temperature storage can accelerate the dissociation rate of each solution, and greater amount of hydrogen ions dissociates from the solution and interact with the silicon MC plate surface. But low-temperature storage may slow down this reaction.
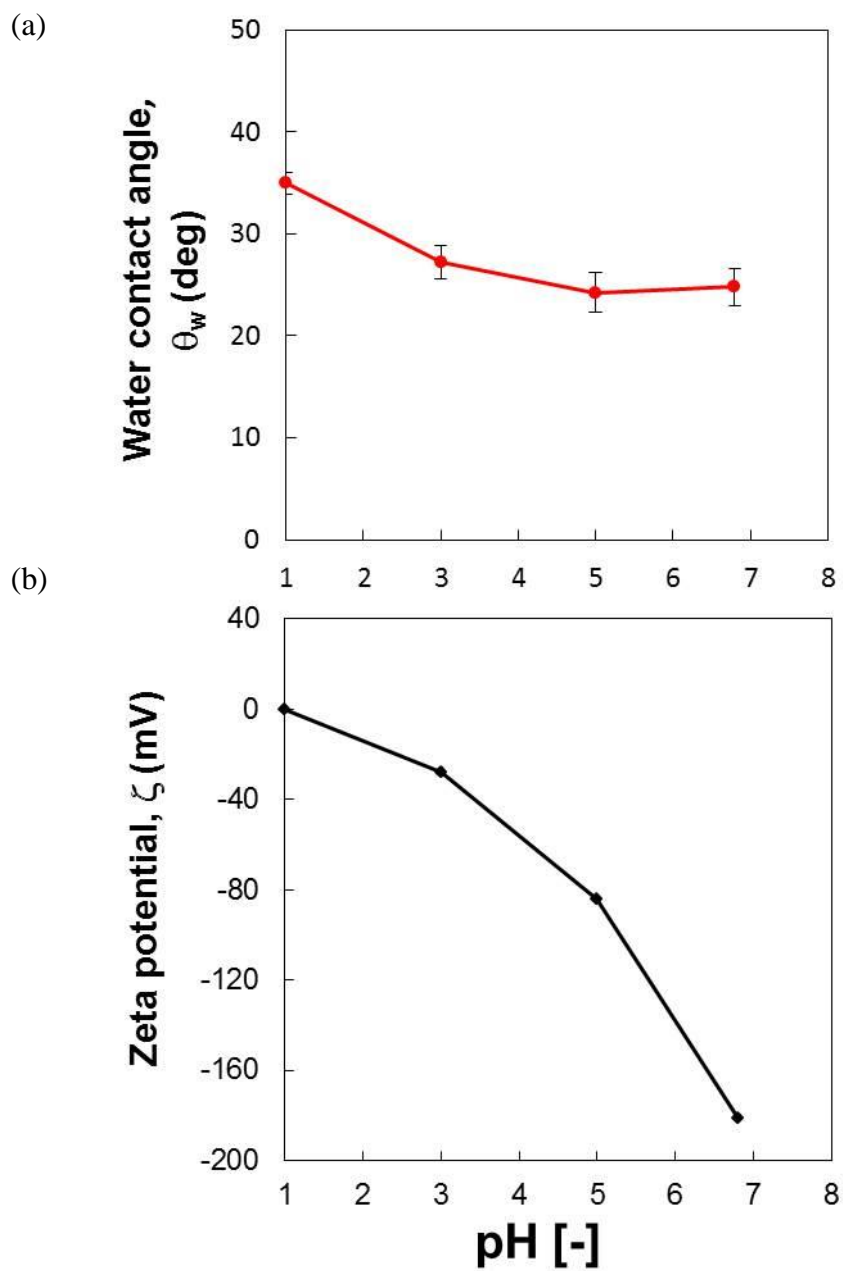
(a)

(b)

Figure 2-7 (a) Variation of water contact angle to silicon MC plates stored in nitric acid as a function of pH. (b) Surface zeta potential of MC plate and variation of water contact angle to silicon MC plates stored in nitric acid as a function of different pH values.

This interaction can be considered as a physical adsorption; because of silica is a porous material that after a continuous adsorption process the most pores will filled with hydrogen irons and some other molecular that were adsorbed. This may be the reason of even stored the MC plate in Milli-Q water at low temperature but after one month it somewhat lost its surface hydrophilicity either.

2.3.2 Effect of water contact angle to silicon MC plate on MC emulsification

2.3.2.1 Dynamic contact angle to MC wall

Fig. 2-8 presents the dynamic contact angle data to the MC wall obtained by the MC array method. For the tween 20-containing system, the MC plate stored for >1 year with a 80° static water contact angle had an advancing dynamic contact angle of 156° and a receding dynamic contact angle of 123° . The difference between the advancing and receding contact angles was quite large. The preceding results suggest that the large difference between the advancing and receding contact angles is due to that the MC plate after the long-term storage almost loses its surface hydrophilicity. In contrast, the similar advancing and receding dynamic contact angles were obtained when using the MC plate with a static water contact angle of 10° just after surface treatment. When the MC plate with a water contact angle of 30° or 60° were used, there were slight differences between the advancing and receding dynamic contact angles. Butron Fujiu *et al.* (2011b) reported that the oil-in-water systems with a dynamic contact angle of about 140° was high enough to produce monodisperse O/W emulsions. For the SDS-containing system, the MC plate stored for >1 year with a 80° static water angle had an advancing dynamic contact angle somewhat higher than a receding dynamic contact angle (Fig. 2-8b). These dynamic contact angles were   higher than 140° . The preceding results suggest that the use of an anionic emulsifier (SDS) reduced the difference of the
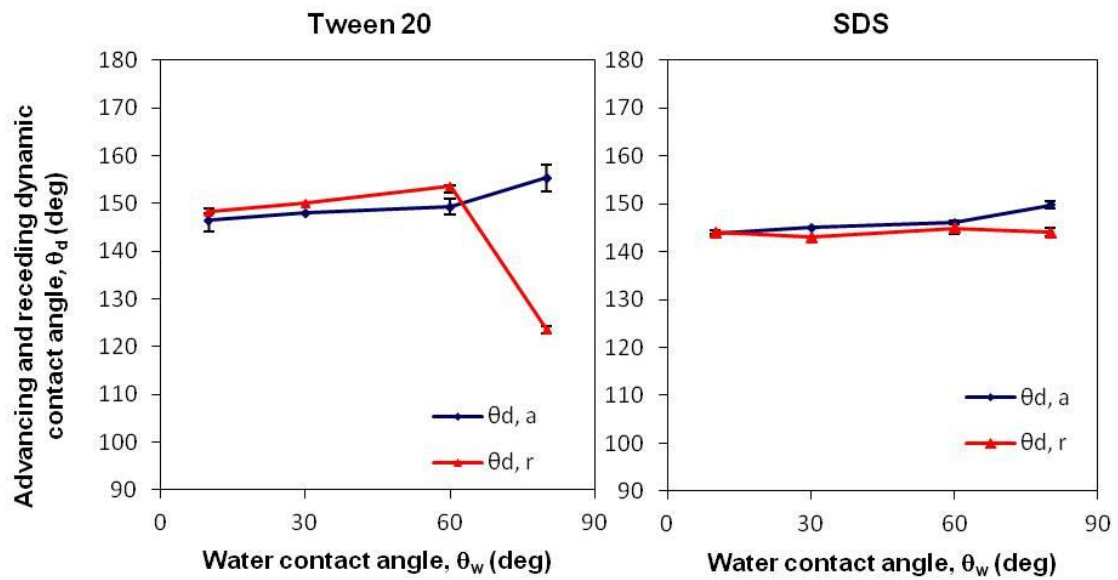
Figure 2-8 Variation of the dynamic advancing and receding contact angles to the MC wall for the Tween 20-containing system and SDS-containing system as a function of θ_w.

advancing and receding dynamic contact angles. In contrast, similar advancing and receding dynamic contact angles were obtained when using the MC plate with water contact angle of 10° just after surface treatment. When the MC plate with a water contact angle of 30° or 60° were used, there were almost no change between the advancing and receding dynamic contact angles. In MC emulsification, the dynamic contact angle is a key parameter affecting droplet generation from channels (Kawakatsu et al., 2001; Kobayashi et al., 2009).

2.3.2.2 Oil droplet generation from rectangular MCs

Fig. 2-9a depicts typical micrographs of droplets generation of Tween 20-stabilized droplets from the channels. The gradually pressurized dispersed phase started to pass through the MCs at a breakthrough pressure ($\Delta P_{d,bt}$) of 2.4 kPa, when the oil droplets generation began. The micrographs (ⅰ) to (ⅲ) demonstrate stable droplet generation using the MC plate just after surface treatment with a 10° static water contact angle. The oil-water interface covered by Tween 20 moved smoothly in the channel and in the well during droplet generation, and the interfacial shape was symmetric to the center line of each channel. The micrographs (ⅳ) to (ⅵ) demonstrate unstable droplet generation using the MC plate just after storage for >1 year with a 80° static water contact angle. The oil-water interface covered by Tween 20 had an asymmetric shape near the channel outlet, and the interface partly wetted on the MC wall. The interfacial movement on the channel and in the well was also not smooth. These behaviors may be caused by some affinity between the dispersed phase covered by the nonionic emulsifier and the MC plate surface. Fig. 2-9b depicts optical micrographs of the generation of SDS-stabilized droplets from the channels. Droplet generation via channels began at a $\Delta P_{d,bt}$ of 2.2 kPa. The micrographs (ⅰ) to (ⅲ) demonstrate stable droplet generation using the MC plate
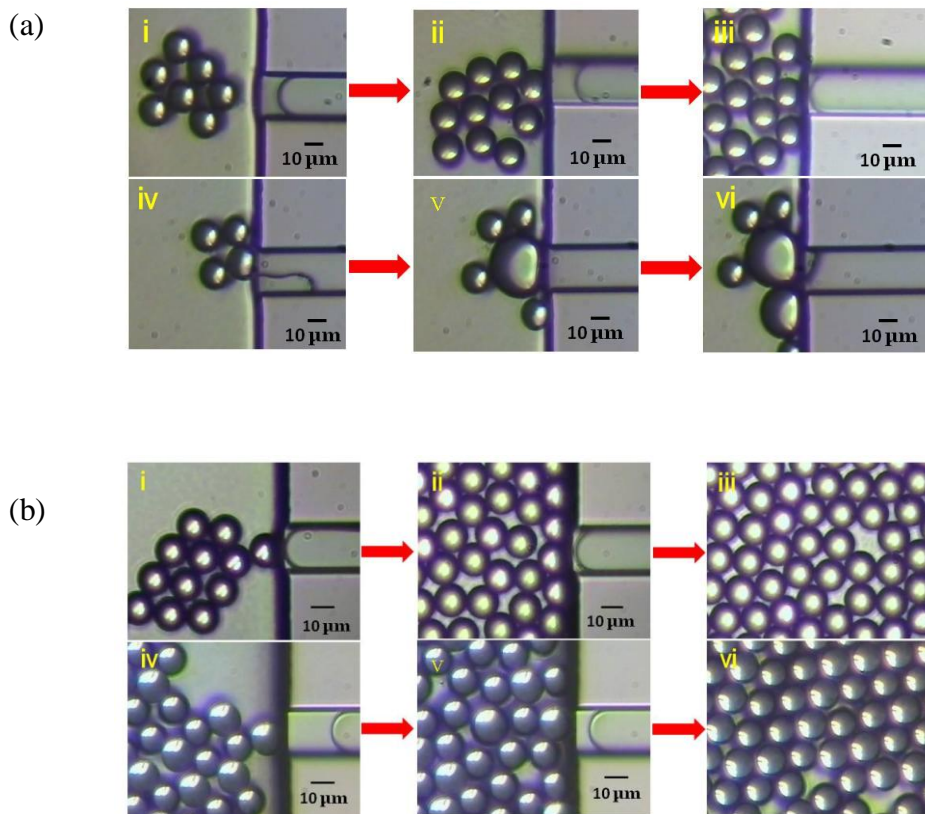
Figure 2-9 (a) Typical optical micrographs of generation of oil droplets stabilized by Tween 20 from channels. i to iii MC plate just after surface treatment. d to f MC plate stored in air for >1 year. (b) Typical optical micrographs of oil droplets stabilized by Tween 20 from the channels. i to iii MC plate just after surface treatment, iv to vi MC plate stored in air for > 1 year.

just after surface treatment. The oil-water interface covered by SDS moved smoothly in the channel and in the well during droplet generation, and the interfacial shape was symmetric to the center line of each channel. The micrographs（ⅵ）to（ⅳ）also demonstrate that droplet generation from the channels seems to be smooth. The oil-water interface stabilized by SDS molecules has a strongly repulsive interaction to the negatively charged channel surface, preventing wetting of the dispersed phase to the MC plate surface (Tong et al., 2000; Kobayashi et al., 2003; Butron et al., 2011a).

Fig. 2-10 presents the effect of the water contact angle to the MC plate on the droplet size and droplet size distribution. In Tween 20-containing system, $d_{n, drop}$ ranged from 15.1 to 22.2 μm. $d_{n,drop}$ was not influenced by the static water contact angle in its range of $<60°$. The CV of the resultant droplets ranged from 2.6% to 20.7%. Such droplet size distribution data demonstrate that monodisperse O/W emulsions were produced using the MC plates with a water contact angle of $<60°$ and that polydisperse O/W emulsion was prepared using the long-term stored MC plate with a water contact angle of $80°$. These results indicate that keeping a low water contact angle is important to produce monodisperse emulsions; i.e., keeping the channel surfaces hydrophilic is required for successful MC emulsification (Tong et al., 2000; Kobayashi et al., 2002b). The droplet produced by SDS-containing system had a $d_{n,drop}$ range from 14.1 to 15.7 μm. $d_{n,drop}$ was slightly influenced by the water contact angle in its range applied. The CV of the resultant droplets ranged from 2.3% to 9.3%. Such droplet size distribution data demonstrate that monodisperse O/W emulsions were produced with a water contact angle of $10°$ to $80°$. Although the dynamic contact angle obtained here are considered to be high enough to prevent unfavorable wetting of the dispersed phase to the plate surface, the difference between the advancing and receding dynamic contact angles may cause generation of slightly polydisperse droplets using the long-term stored MC plate.
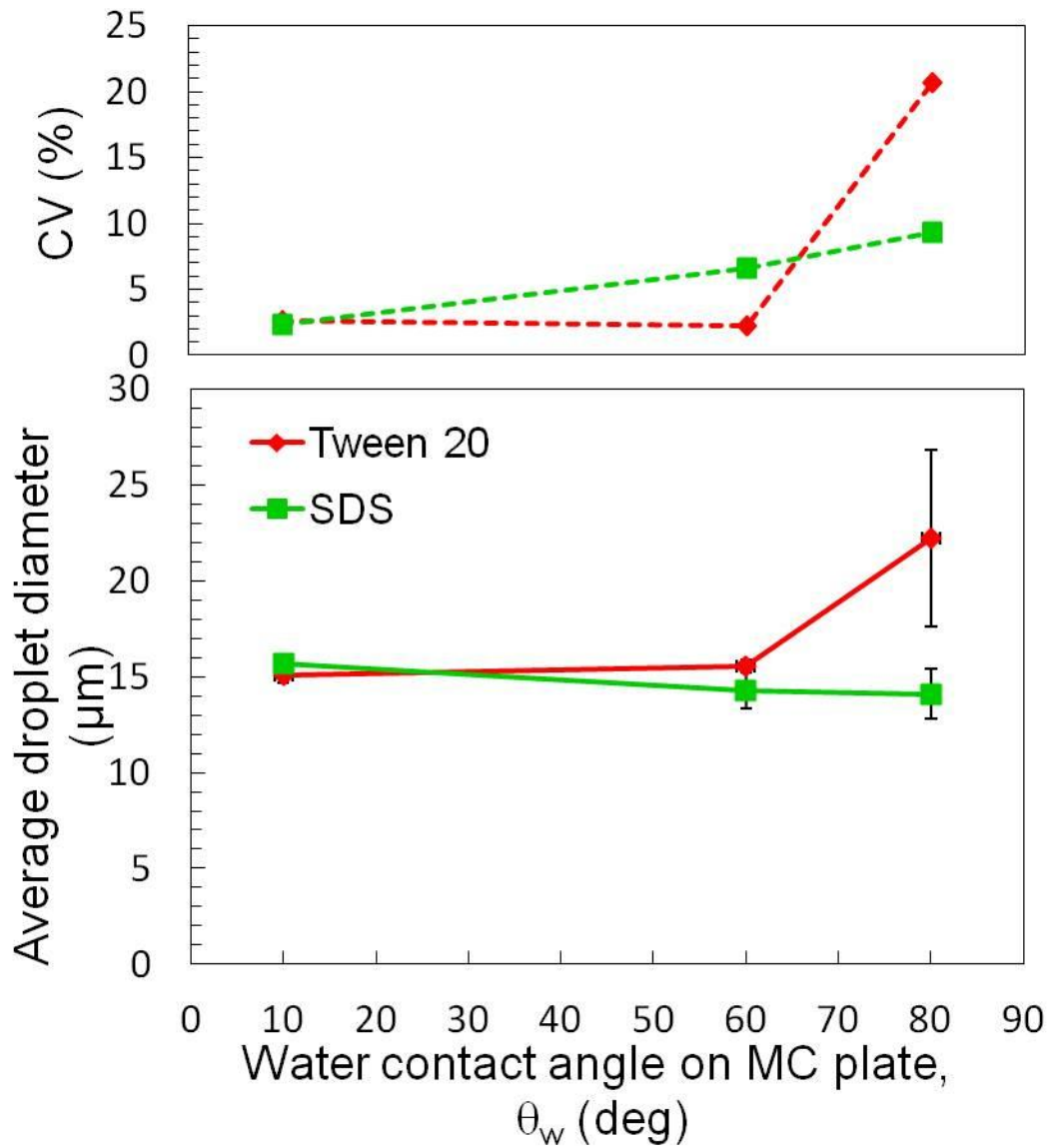
Figure 2-10 Variation of the average droplet diameter and CV of the produced emulsions as a function of the water contact angle to MC plate.

2.4 Conclusions

The surface-treated silicon MC plates gradually lost their hydrophilicity in time, which is influenced by storage conditions such as medium and temperature. Moreover, the hydrophilic property of the plasma treated silicon MC plate was better kept by storing in a hydrophilic medium with negatively charged MC plate surface due to a low concentration of positively charged hydrogen ions. The effect of the MC plate surface properties on droplet generation results elucidated that monodisperse food-grade O/W emulsions can be produced when using a silicon MC plate with a static water contact angle below a critical value and above a critical value of dynamic contact angle inside the MC. Our results could give some information useful for optimized operation of MC emulsification.

Chapter 3

Droplet Generation Behavior During Continuous MC

Emulsification

3.1 Introduction

Emulsions containing droplets dispersed within a continuous phase play an important role in the production of foods, cosmetics, pharmaceuticals, and chemicals (Mason *et al.,* 1996). In particular, monodisperse emulsions containing uniformly sized droplets can improve stability against droplet coalescence and allow simplified interpretation of experimental results, as well as enable the precise control of some emulsion properties (Mason *et al.,* 1996; McClements, 2004). However, traditional emulsification techniques, that apply intensive forces to break down larger droplets into smaller ones, generally produce polydisperse emulsions difficult to satisfy the requirements for desired emulsion properties (McClements, 2004).

Microfabricated emulsification devices that enable producing relatively monodisperse emulsions have been developed over the past two decades (Vladisavljević *et al.*, 2012). Membrane emulsification, proposed by Nakashima *et al.* (1991), is capable of producing relatively uniform emulsion droplets with the smallest coefficient of variation (CV) of approximately 10%, which is primarily due to the size distribution of membrane pores. In direct membrane emulsification, droplets are generated by pressurizing a dispersed phase through membrane pores into a continuous phase, and the resultant droplet size ranging between 0.3 and 60 μm can be controlled by the pore size (Nakashima *et al.*, 1991; Vladisavljević *et al.*, 2002). Kawakatsu *et al.* (1997) proposed microchannel (MC) emulsification that enables producing uniform emulsion droplets with average diameters of 1 to 200 μm and the smallest CV below 5% (Kobayashi *et al.*, 2007; 2010a). MC emulsification has a unique droplet generation process in which droplets are generated by simply forcing a dispersed phase through an MC array into a continuous phase whose flow is not forced (Kawakatsu *et al.,* 1997;

Kobayashi *et al.,* 2005). Sugiura *et al.* (2001) proposed a spontaneous-transformation-based droplet generation mechanism in MC emulsification that exploits interfacial tension dominant on a micron scale. This droplet generation requires low energy input (typically 10^3-10^4 J/m^3) and is very mild (Sugiura *et al.*, 2001), which is advantageous for preventing the degradation of shear- and heat-sensitive food components. Food-grade triglyceride oils and emulsifiers have been used for MC emulsification in order to produce monodisperse oil-in-water (O/W) and water-in-oil (W/O) emulsions (Kobayashi *et al.*, 2011). Seemingly, monodisperse O/W emulsions loaded with functional lipids have been produced by MC emulsification (Kobayashi *et al.*, 2011). The monodisperse food-grade emulsions produced by MC emulsification have also been applied to produce monodisperse solid and gel microparticles, besides monodisperse microcapsules (Kobayashi *et al.*, 2011).

Long-term continuous MC emulsification is a key factor for achieving practical-scale production of monodisperse emulsions. Tong *et al.* (2002) demonstrated a successful short-term production of a monodisperse oil-in-water (O/W) emulsion for up to 4 h. However, changes in droplet generation during long-term continuous MC emulsification have not yet been studied. In this study, we conducted long-term continuous production of O/W emulsions by MC emulsification for up to 7 days. We investigated the effects of the operation time and surfactant type on the generation characteristics of emulsion droplets using a hydrophilically treated silicon MC array plate.

3.2 Materials and Methods

3.2.1 Materials

Refined soybean oil, sodium dodecyl sulfate (SDS, hydrophilic lipophilic balance (HLB): 40), and polyoxyethylene (20) sorbitan monolaurate (Tween 20, HLB: 15) were purchased from Wako Pure Chemical Industries Ltd. (Osaka, Japan). The water used in this study was filtered deionized water (Milli-Q water).

3.2.2 Long-term continuous MC emulsification

Figure 3-1a schematically depicts the experimental setup used for long-term continuous MC emulsification. It is composed of a module equipped with a silicon MC array plate (model CMS 6-2) (Chuah *et al*., 2009), a 10-mL liquid chamber for supplying a dispersed phase, a 1-L tank for supplying a continuous phase, and a microscopic video system (Kobayashi *et al*., 2010b). Figure 1b schematically depicts the CMS 6-2 plate having 10 MC arrays fabricated through a process of photolithography and orientation-dependent wet etching. Each MC array consists of 107 parallel MCs (4-μm depth, 8-μm width, 140-μm length) and terraces (4-μm depth, 40-μm length) outside MC inlets and outlets. Deeply etched channels (100-μm depth) for flowing liquid phases are located outside the MC array. Prior to the first use, the MC array plate was subjected to plasma oxidization using O_2 gas (PR500, Yamato Scientific Co., Ltd., Tokyo, Japan) at an internal chamber pressure of 15 Pa for 15 min in order to render its surfaces hydrophilic.

In MC emulsification experiments, we used refined soybean oil as the dispersed phase and a Milli-Q water solution containing SDS or Tween 20 (1.0 wt%) as the continuous phase. When assembling the module, the MC array plate was tightly attached onto a flat glass plate, and its internal compartments were filled with the continuous phase. After connecting the liquid chamber to the module via a flexible tube,
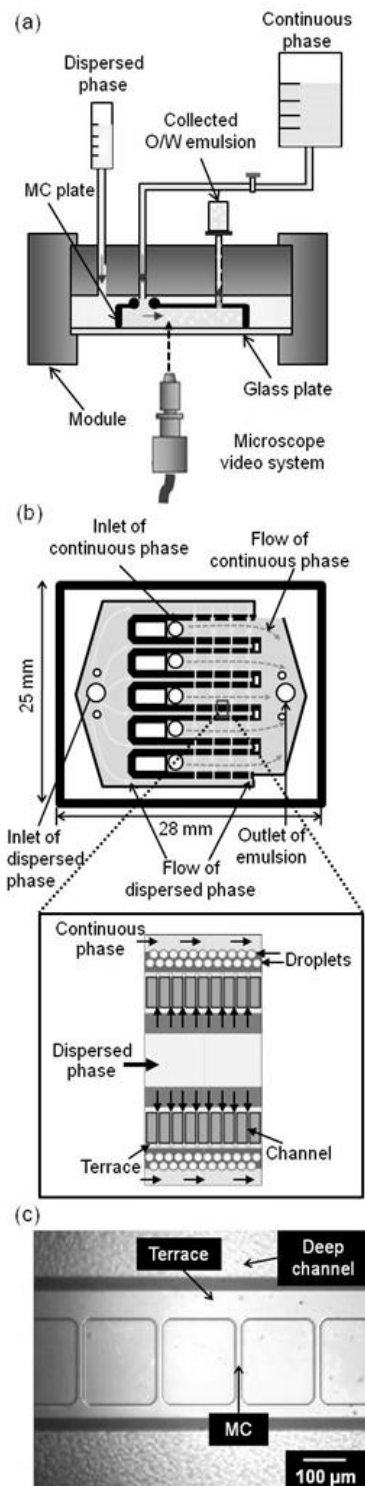
Figure.3-1 (a) Schematic cross-sectional view of MC emulsification setup. (b) Schematic top views of a silicon MC array plate (model CMS 6-2) and droplet generation via MCs. (c) Optical micrograph of part of an MC array.

the dispersed phase pressurized by lifting the chamber was introduced into the module. The pressure applied to the dispersed phase (ΔP_d) was determined by the following equation (Kobayashi *et al*., 2009):

$$\Delta P_d = \rho_d \Delta h_d g \tag{1}$$

where ρ_d is the dispersed-phase density (920 kg/m^3 for soybean oil), Δh_d is the difference in the hydraulic heads between the liquid chamber and the MC array plate, and g is the acceleration due to gravity. To generate oil droplets, the dispersed phase was forced to pass through MC arrays in a precisely controlled manner. The generated droplets were slowly swept away by the cross-flow of the continuous phase (3.8 mL/h). All experiments were carried out at a room temperature (~25°C). Droplet generation during continuous MC emulsification was monitored and recorded every 24 h up to 7 days using the microscope video system.

3.2.3 Determination of average droplet diameter

The microscopic images of the generated droplets captured in a computer were used for measuring their diameter. The average diameter (d_{av}) of the generated droplets was determined from the diameter data of 100 droplets measured using image analysis software (WinRoof version 5.6, Mitani Co., Fukui, Japan). CV used as an indicator of droplet size distribution was calculated by:

$$CV = (\sigma/d_{av}) \times 100 \tag{2}$$

where σ is the standard deviation of the droplet diameter.

3.3 Results and Discussion

The production characteristics of O/W emulsions during long-term continuous MC emulsification are reported below. Figure 3-2a(i) depicts a typical micrograph of droplet generation via part of an MC array on day 1 when using the two-phase system containing SDS. The gradually pressurized dispersed phase started to pass through the MCs at a breakthrough pressure ($\Delta P_{\text{d,bt}}$) of 0.42 kPa, when the oil droplets generation began. The droplets formed were uniformly sized and spherical, and were swept away by the cross-flowing continuous phase in the deep channel. The oil-water interface stabilized by SDS molecules on the terrace repeated smooth expansion and shrinkage during droplet generation cycles. As depicted in Fig. 3-2b(i), the interfacial shape was kept symmetric to the center line of the MC. These results are typical behaviors for successful, stable droplet generation by MC emulsification (Butron Fujiu *et al*., 2011a). Figure 3-3a illustrates the variation of the d_{av} and CV of the resultant O/W emulsion droplets stabilized by SDS during the continuous MC emulsification. The oil droplets obtained on day 1 had a d_{av} of 23.2 μm and a CV of 2.1% and a highly narrow size distribution with a monomodal sharp peak (Fig. 3-3b(i)), demonstrating the production of a monodisperse O/W emulsion. Droplet generation via MC arrays did not change during 7 days of continuous MC emulsification (Fig. 3-2a). Moreover, the smooth and symmetric motion of the oil-water interface repeated on the terrace was observed on days 3, 5, and 7 (Fig. 3-2b). The d_{av} and CV of the generated droplets were almost unaffected by the operation time (Fig. 3-3a). In this case, their d_{av} ranged between 21.5 and 23.2 μm, and their CV ranged between 2.1 and 3.6%. The highly narrow droplet size distributions remained up to day 7. These results demonstrate that continuous MC emulsification using the two-phase system containing SDS is capable of stably
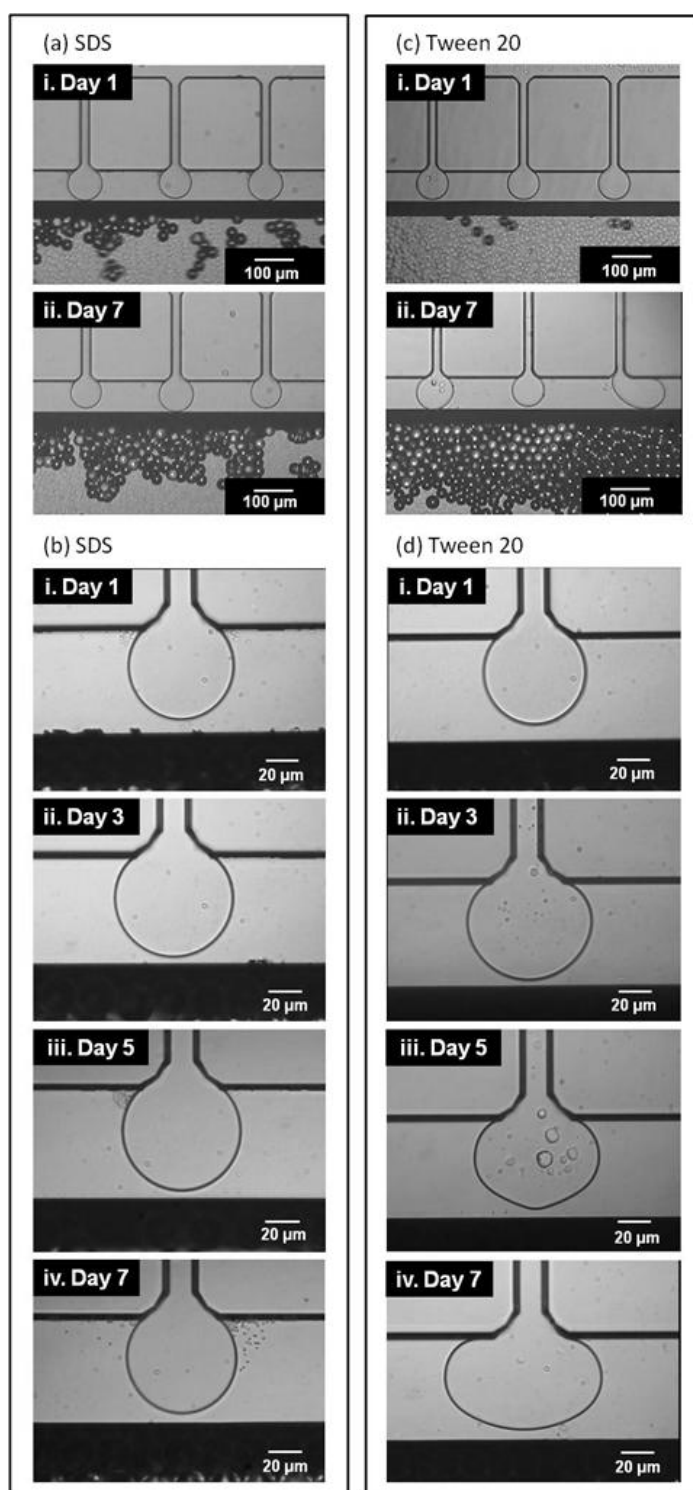
Figure 3-2 (a, c) Optical micrographs of oil droplet generation from the MCs. (b, d) Optical micrographs of the dispersed phase expanding on the terrace. (a, b) SDS. (c, d) Tween 20.
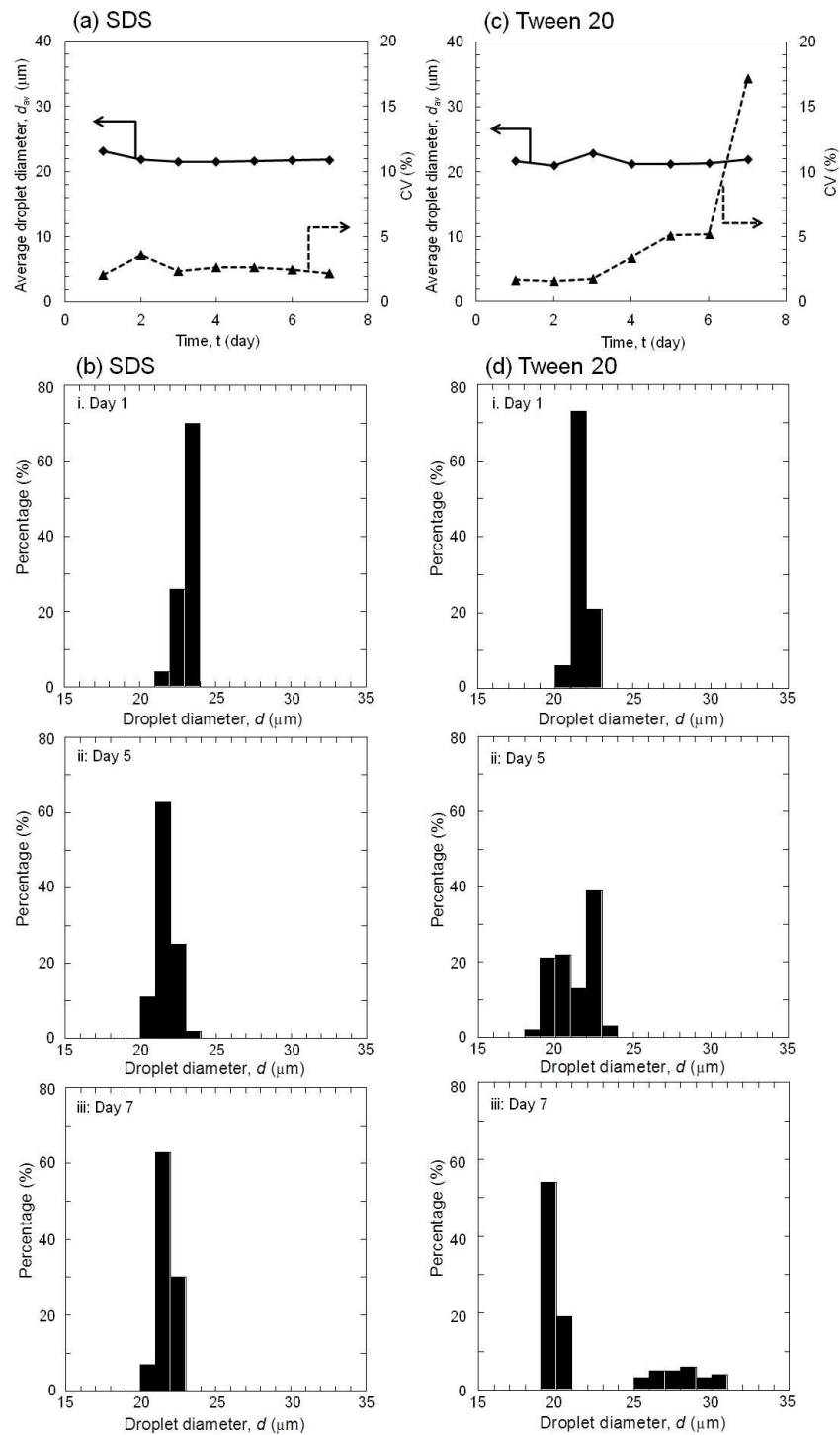
Figure 3-3 (a, c) Variations in the d_{av} and CV of the O/W emulsion droplets obtained during long-term continuous MC emulsification as a function of time. (b, d) Size distributions of the resultant O/W emulsion droplets. (a, b) SDS. (c, d) Tween 20.

producing monodisperse O/W emulsions for at least 7 days. This successful long-term MC emulsification could be attributed to the strong repulsive forces functioning between anionic SDS molecules that cover the oil-water interface and negatively charged chip surfaces due to the presence of silanol group. Kobayashi *et al*. (2012) recently reported the highly negative ζ-potential values of soybean oil droplets stabilized by SDS and the chip surface. Our result also indicates that this strong repulsive interaction can be kept for at least 7 days.

Figure 3-2c(i) depicts a typical micrograph of droplet generation via part of an MC array on day 1 when using the two-phase system containing Tween 20. At a $\Delta P_{d,bt}$ of 0.54 kPa, oil droplet generation began from some of the MCs. The fresh spherical droplets of uniform size were swept away in the deep channel in the presence of the cross-flowing continuous phase. The oil-water interface stabilized by Tween 20 molecules on the terrace repeated symmetric expansion and shrinkage during droplet generation cycles. As depicted in Fig. 3-2d(i), successful, stable droplet generation cycles were observed on day 1. Figure 3-3c illustrates the variation of the d_{av} and CV of the resultant O/W emulsion droplets stabilized by Tween 20 during the continuous MC emulsification. On day 1, the d_{av} and CV of the oil droplets were 21.6 μm and 1.7%, respectively. A highly narrow droplet size distribution with a monomodal sharp peak (Fig. 3-3d(i)) demonstrates the production of a monodisperse O/W emulsion. However, the oil-water interface on the terrace started to become asymmetric to the center line of the MC and greater on day 3 (Fig. 3-2d(ii)). Moreover, the motion of this interface became less smooth during droplet generation cycles. Afterwards, the oil-water interface on the terrace deformed more asymmetrically on day 7, indicating wetting of the dispersed phase on part of the terrace surface (Fig. 3-2d(iv)). The d_{av} of the

generated droplets were slightly affected by the operation time and ranged between 21.2 and 22.9 μm (Fig. 3-3c). Their CV values were below 2% on days 1 to 3, gradually increased up to about 5% on days 4 to 6, and became remarkably higher, reaching up to 17.2% on day 7. Moreover, the droplet size distributions in Fig. 3d became broader on day 5, and had bimodal peaks on day 7, indicating the production of a polydisperse O/W emulsion on day 7.

Butron Fujiu *et al.* (2011a; 2011b) reported that the maximum generation rate of uniformly sized soybean oil droplets stabilized by nonionic Tween 20 is quite lower than those stabilized by anionic SDS when using a hydrophilic silicon MC array plate. Kobayashi *et al.* (2012) also reported some affinity between the dispersed phase covered by Tween 20 molecules and the plate surface, as the absolute ζ-potentials of soybean oil droplets stabilized by Tween 20 and the chip surface are pronouncedly lower than those for the SDS-containing system. We assume that the affinity interaction between the oil-water interface in the presence of Tween 20 and the terrace surface made the oil-water interface asymmetric on days 3 to 7, because of their lower absolute ζ-potentials as well as a very thin layer of the continuous phase that exists between them. This slowly increasing affinity interaction may have caused the variations of the droplet generation behavior (Figs. 3-2c, d) and droplet size distribution (Fig. 3-3d).

The MC emulsification results obtained from this study have demonstrated that monodisperse O/W emulsions were successfully and continuously produced for up to 7 days when the strong repulsive force functions between the dispersed phase covered by emulsifier molecules and the MC and terrace surfaces. Our results also suggest that appropriate selection of emulsion composition including the emulsifier type is essential to achieve successful long-term continuous MC emulsification. The findings are

expected to provide useful information about the long-term continuous production of monodisperse emulsions as templates for monodisperse microparticles and microcapsules using MC emulsification.

3.4 Conclusions

This chapter has demonstrated droplet generation behaviors during continuous MC emulsification using different emulsifiers. The time course of the water contact angle to the MC plate under storage conditions that imitate continuous MC emulsification was first investigated. During 7 days of storage in the dispersed phase, the water contact angle was maintained $<30^{o}$. This result indicates that a very thin layer of emulsifier molecules on the plate surface can prevent wetting of the dispersed phase on the plate surface. The following findings were also obtained from continuous MC emulsification up to one week. For the Tween 20-containing system, the average diameter of the generated oil droplets slightly increased with time, and their CV gradually increased in time. On days 5 to 7, there was some affinity between the dispersed phase covered by the nonionic emulsifier and the plate surface. For the SDS-containing system, monodisperse oil droplets with CV below 5% were obtained during 7 days of operation, with a negligible change of their average diameter and CV. These results are supposed to be due to the strongly repulsive force between the dispersed phase covered by negatively charged SDS molecules and the negatively charged silanol group formed on the MC plate.

Chapter 4

Development of Asymmetric Metal Straight-through Microchannel Arrays and Evaluation of its Production Characteristics

4.1 Introduction

Emulsification technologies that generate droplets dispersed in a continuous phase play an important role in the production of foods, cosmetics, pharmaceutical and chemical industries (Mason et al., 1996). Monodisperse emulsions containing uniformly sized droplets can improve the stability against droplet coalescence and allow simplified interpretation of experimental results, in addition to precise control over some emulsion properties (Mason et al., 1996; McClements et al., 2004). The traditional emulsification techniques apply intensive forces to break down larger droplets into smaller ones, generally produce polydisperse emulsions, which have low storage / physical stability (McClements et al., 2004).

Microfabricated emulsification devices that have the potential to produce comparatively monodisperse emulsions have been developed over the past two decades (Vladisavljević et al., 2012). Microfabricated emulsification devices with different structures, such as T-junction (Thorssen et al., 2001; Yi et al., 2003), cross-junction (Nisisako et al., 2004; Tan et al., 2006) and Y-junction (Steegmans et al., 2009) can generate extremely monodispersed single, double, triple or multiple emulsions with droplet size larger than 10 μm, in a single step. Microfabricated emulsification devices can be applied in many fields, but for generic use, the low productivity of such devices should be improved. Nakashima *et al*. (1991) reported an emulsification technique, named as membrane emulsification, which, due to the relatively narrow size distribution of membrane pores could produce relatively uniform emulsion droplets with the smallest CV of approximately 10%. In direct membrane emulsification, droplets are generated by pressurizing a dispersed phase through membrane pores into a continuous phase, and the resultant droplet size ranging between 0.3 and 60 μm can be controlled

by the pore size (Nakashima *et al.*, 1991; Vladisavljević et al., 2002). Vladisavljević and Williams (2006) investigated the production of O/W emulsions by rotating membrane emulsification, using stainless-steel membrane with pore size of 100 μm. This system is capable of producing monodispersed oil droplets with d_{av} up to 107 μm and CV less than 5%.

Microchannel (MC) emulsification is a promising and progressive technique to produce monodisperse emulsions (Kawakatsu et al., 1997; Kobayashi et al., 2005). Droplet generation in MC emulsification is a unique and mild process driven by interfacial tension on a micron scale (Sugiura et al., 2001; Kobayashi et al., 2011). Monodisperse oil-in-water (O/W) and water-in-oil (W/O) emulsions with the smallest CV below 5% have been prepared through this emulsification process (Kawakatsu et al., 1997; Kawakatsu et al., 1999; Kobayashi et al., 2001; Sugiura et al., 2002).

MC emulsification devices can be categorized into two types either grooved MC arrays or straight-through MC array (Kawakatsu et al., 1997; Kawakatsu et al., 1999). Grooved MC array consists of uniform microgrooves and a slit-like terrace. This type is used to study the droplet production characteristics by easy observation of the water-oil interface movement inside the MC arrays. Straight-through MC arrays consist of uniform, symmetric or asymmetric micro-hole with circular holes and micro-slots (Kobayashi et al., 2002; Kobayashi et al., 2004; Kobayashi et al., 2005). In contrast to grooved MC arrays, straight-through MC arrays have much higher droplet production rates, but direct observation and characterization inside straight-through holes is difficult.

MC emulsification chips are normally made of silicon-based materials (Kawakatsu et al., 1997; Sugiura et al., 2001), which are superior in terms of precise machining of

MC arrays with uniform-sized channels. However, silicon chips have few drawbacks, such as shock fragility and intolerance against alkali cleaning. Aluminum and stainless-steel are practically more suitable materials due to chemical-proof surfaces and superior mechanical strengths. The superior mechanical strength of these two materials is also suitable for handling and repeated use of these chips for longer period of time.

Tong developed a grooved MC array consisting of only parallel channels on a stainless-steel chip capable of producing monodispersed droplets with diameter ranging from 20 to 210 μm. The channels fabricated individually by microcutting lacked precisely uniform size, confirming the difficulty to obtain monodisperse emulsions using stainless-steel chips.

Recently, Kobayashi developed a stainless-steel MC array consisting of precisely microfabricated parallel channels and a terrace. It had the potential of producing highly monodisperse O/W emulsions with droplets diameter ranging from 350 μm to 570 μm, and CV below 1% with several milliliters per hour scale of droplet productivity.

Kobayashi et al. (2012) also reported the mass production of uniformly sized droplets on a liter per hour scale using a large MC emulsification device, capable of producing uniform sized oil droplets with average diameter of 87 μm and CV below 2%. Application of MC emulsification in industrial production requires not only large scale MC device development, but also needs to consider the generic use of the MC array chips of various materials. The need for generic use of metallic MC arrays with mass production ability has been arising. Prior to developing large scale metallic MC arrays, the droplet generation characteristics of metallic asymmetric straight-through MC array chip should be investigated. Thus, at first aluminum asymmetric straight-through MC array chips, each of them consisting of a precisely microfabricated asymmetric

straight-through geometry in one plate, were developed. The characteristics of droplet generation, size and size distribution of the generated oil droplets and the effect of dispersed phase flow rate on droplet generation were investigated. The dispersed phase flow during droplet generation was also analyzed using dimensionless number. The results obtained in this study provided information for the development of large scale metallic MC emulsification device.

4.2 Materials and methods

4.2.1. Metallic asymmetric MC array chip

Asymmetric MC array chips made of aluminum (WMS-Al) were designed for this study (Fig. 4-1). An asymmetric MC array consists of 30 pair of circular microholes and microslots and compactly arranged within a 10×10-mm central area of the 24×24-mm chip. Polished aluminum chips [Japanese Industrial Standard (JIS) A5052] were subjected to a micromachining process. Each asymmetric MC array was microfabricated through end milling for forming circular microholes and subsequent electric discharge machining for forming microslots connected to microholes. Part of the metallic asymmetric MC arrays after microfabrication is depicted in Fig. 4-1c and d. Their geometric characteristics are presented in Table 1. The microfabricated circular microholes and microslots were nearly within the designed sizes and shapes. An oxide layer (Al_2O_3) on the microfabricated chip surface was formed using anodizing. Prior to the first use for MC emulsification, the WMS-Al chips were surface-oxidized once again with an oxygen plasma reactor (PR500, Yamato Scientific Co., Ltd., Tokyo, Japan) for 10 min at 15 Pa.

4.2.2. Materials

Refined soybean oil was used as dispersed phase. Polyoxyethylene (20) sorbitan monolaurate (Tween 20, hydrophilic lipophilic balance (HLB): 15) was used as emulsifier. They were purchased from Wako Pure Chemical Industries Ltd. (Osaka, Japan) and were used as received.

4.2.3. Droplet generation by MC emulsification

Figure 4-2 schematically shows the experimental setup for MC emulsification used in this study. It consists of the module equipped with a metallic asymmetric MC array chip, a syringe pump (Model 11 plus; Harvard Apparatus, Inc., Holliston, USA) equipped with a 20-mL glass syringe for supplying the dispersed phase, a 1-L tank for supplying the continuous phase and a microscopic video system [25].

A continuous-phase solution was prepared by dissolving an emulsifier into Milli-Q water at a concentration of 1.0 wt%. The MC array chip soaked in the continuous phase was initially degassed by ultrasonication at 100 MHz (VS-10III, As One Co., Osaka, Japan). For module assembly, the metallic chip was mounted inside the compartment filled with the continuous phase. The dispersed phase was breathed into the MC array at a controlled flow rate (Q_d) ranging from 0.5 mL h^{-1} to 5 mL h^{-1}. The continuous phase was introduced into the module at a flow rate (Q_c) of 360 mL h^{-1}. The dispersed phase was injected via the MC array into the flow channel for the continuous phase to generate emulsion droplets. These experiments were conducted at 25°C, and the droplet generation was monitored and recorded in real time using the microscope video system.

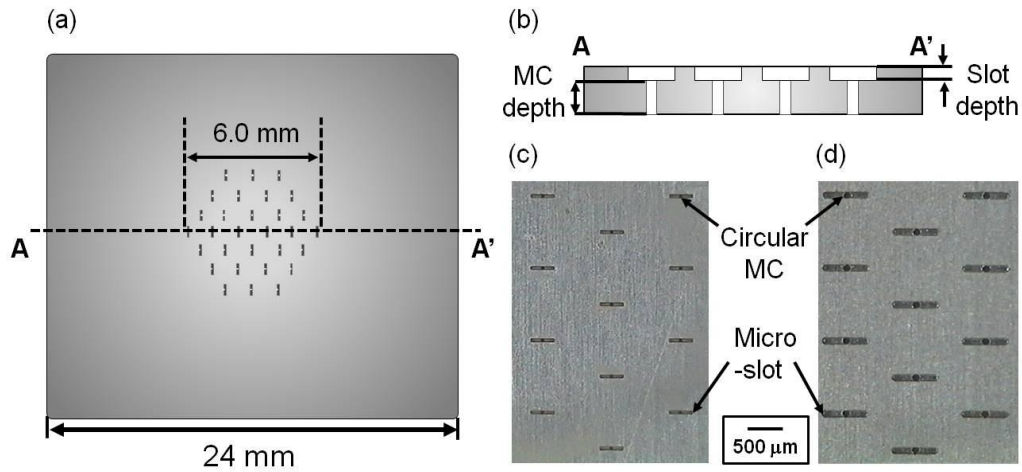4.2.4. Determination of droplet size and droplet size distribution

69

Figure 4-1 (a and b) Schematic representations of a metallic asymmetric straight-through MC array (a) Top view of the chip. (b) Cross-sectional view of the chip. (c and d) Scanning electron micrographs of the outlets of metallic asymmetric through holes (c) WMS-Al-50 (d) WMS-Al-100.

The size and size distribution of the resulting oil droplets were determined by capturing their microscopic images and further processing through image analysis software (WinRoof version 5.6, Mitani Co., Fukui, Japan). The average diameter (d_{av}) was determined by taking the average of 100 droplets and the droplet size distribution factor was calculated as coefficient of variation (CV) through the following equation:

$$CV = (\sigma/d_{av}) \times 100 \qquad (1)$$

where σ is the standard deviation of the droplet diameter.

4.2.5. Contact angle measurement

The static contact angle of an oil drop against the flat chip surface outside an MC array was measured using the contact angle measurement mode of a fully automatic interfacial tensiometer (PD-W, Kyowa Interface Sciences Co., Ltd., Saitama, Japan). The MC array chip was floated on the continuous phase in a transparent cell. An oil drop with a volume of 0.5 μL was then upwards into the continuous phase and contacted the downside of the chip. The static oil contact angle was determined from the captured images of 5 drops by θ/2 method.

4.3 Results and discussion

4.3.1. Droplet generation via metallic asymmetric MC arrays

A typical example of oil droplet generation using asymmetric MCs (WMS-Al-100 chip) is depicted in Fig. 4-3a(i). Refined soybean oil was used as the dispersed phase, and a Milli-Q water containing 1.0 wt% Tween 20 was used as the continuous phase. The droplets were generated at Q_d of 1.0 mL h^{-1} and Q_c of 360 mL h^{-1}. Optical microscopy illustrated the periodic generation of uniform-sized oil droplets with d_{av} of
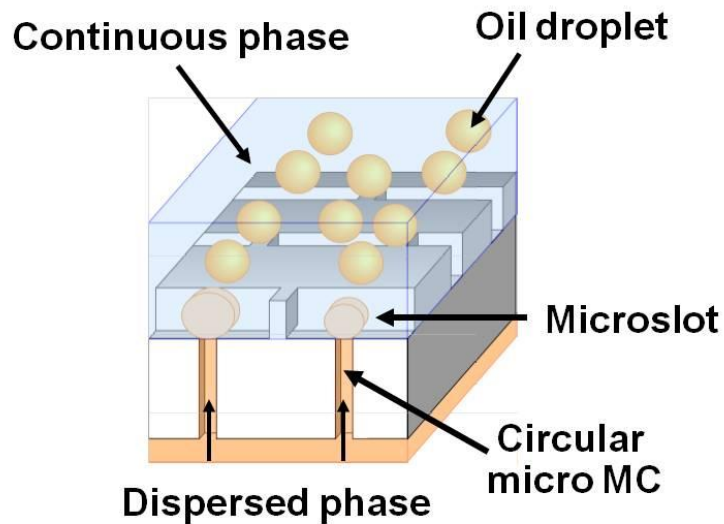
(a)
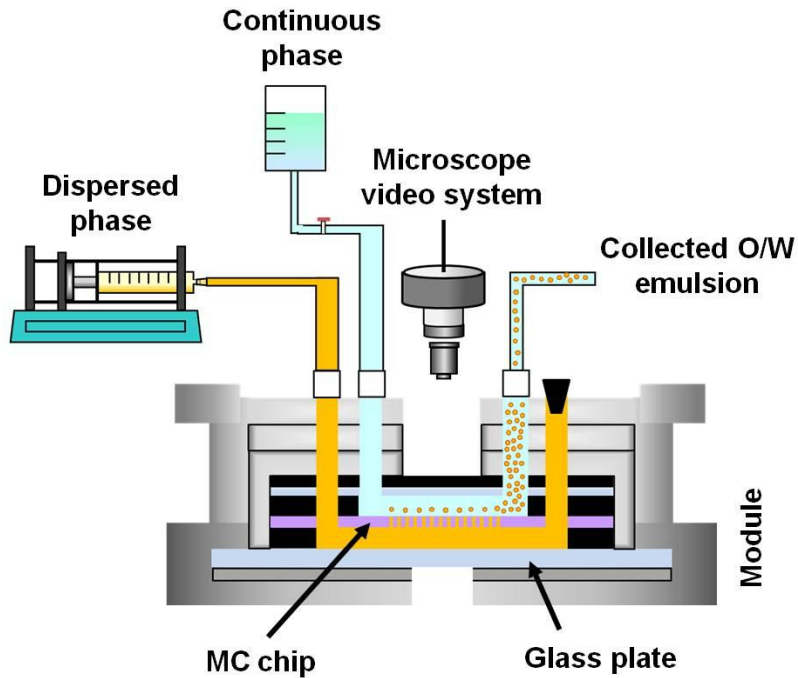
(b)

Figure 4-2 Schematic drawings of the Microchannel emulsification experimental setup used in this study (a) and droplet generation via asymmetric through holes (b). Schematic view of the generation of O/W emulsion droplets via asymmetric straight-through MCs.

293.6 μm from all the microslots. The resulting droplets with CV values around 2.5% had very narrow size distribution with monomodal peak (Fig 4-3a(ii)), confirming the capability of metallic asymmetric MC array chip for producing monodisperse O/W emulsions.

Using the same method described earlier, WMS-Al chip with different microhole diameters (Table 4-1) were used to investigate the effect of size of asymmetric MCs on droplet size and droplet size distribution. The use of WMS-Al-50 chip led to stable generation of smaller oil droplets having d_{av} of 145.6 μm and CV below 4% (Fig. 4-3b(i)). The droplet size distribution presented in Fig. 4-3b(ii) had a monomodal sharp peak, demonstrating the production of a monodisperse O/W emulsion. The droplet size depended greatly on the microhole diameter (d_{MH}) which represents the MC size. The preceding results suggest that monodisperse O/W emulsions with controlled droplet size could be produced using the metallic asymmetric MC arrays developed in this study.

Keeping the chip surface hydrophilic is critical for successfully generating uniform-sized oil droplets by MC emulsification. To evaluate the surface properties of the metallic asymmetric MC array chips, we measured the static contact angle of a soybean oil drop to the chip surface in the presence of a Milli-Q water containing 1 wt% Tween 20. This static contact angle was 126°, indicating that the WMS-Al chips have hydrophilicity lower than silicon MC array chips. It should be noted that monodisperse O/W emulsions can be produced using MC emulsification when the contact angle exceeds about 120°.

4.3.2. Effect of the flow rate of the dispersed phase on droplet generation characteristics
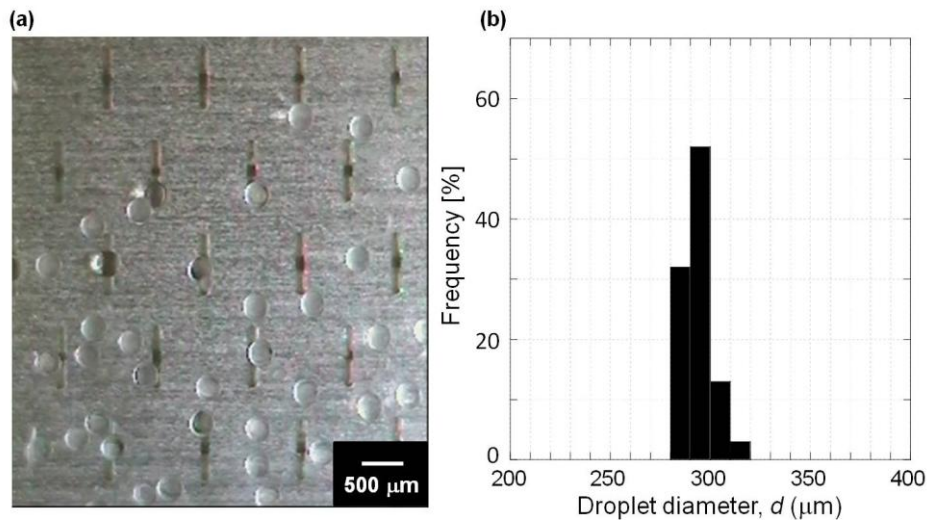
Figure 4-3 (a) Typical droplet generation results using WMS-Al-100 chips. (b) Size distributions of the oil droplets produced using WMS-Al-100.

The effect of Q_d on the size and size distribution of the oil droplets generated using WMS-Al chips was studied by varying Q_d between 0.5 mL h^{-1} and 5 mL h^{-1} with a fixed Q_c at 360 mL h^{-1} As can be seen in Fig. 4-5, we used the dimensionless average droplet size ($\bar{d}$) defined as follows:

$$\bar{d} = \frac{d_{av}}{d_{MH}} \tag{2}.$$

The results show that the $\bar{d}$ and CV of the resulting oil droplets are constant below a critical Q_d, irrespective of d_{MH}. Steep increases in these values occurred above the critical Q_d. The critical Q_d depended clearly on d_{MH}. The critical Q_d values were 1 mL/h for WMS-Al-50 and 3mL/h for WMS-Al-100. This trend would be reasonable, as ideally the critical Q_d increases with increasing to d_{MH} under a fixed MC number(Kobayashi et al., 2011). A previous CFD (computational fluid dynamics) study (Kobayashi et al., 2011) reported that the critical volume-based droplet productivity from each MC is squarely proportional to d_{MH}. Since the WMS-Al chips used in this study have the same MC number (Table 4-1), the calculated difference of the critical Q_d values was 4 times between the WMS-Al chips. This difference is relatively similar to the experimentally obtained difference of three times.

Micrographs in Fig. 4-6a and 6b respectively represent the generation of the oil droplets using the WMS-Al-100 chip below and above the critical Q_d. Below the critical Q_d, the expanding droplet gradually tilted towards the downstream side, and the generated droplets quickly swept away from the slot outlet by the cross-flowing continuous phase (Fig. 4-6a). On the contrary, above the critical Q^d, the expanding dispersed phase did not move towards the downstream area side during droplet generation, and the generated droplets remained attached to the slot outlet (Fig. 4-6b).
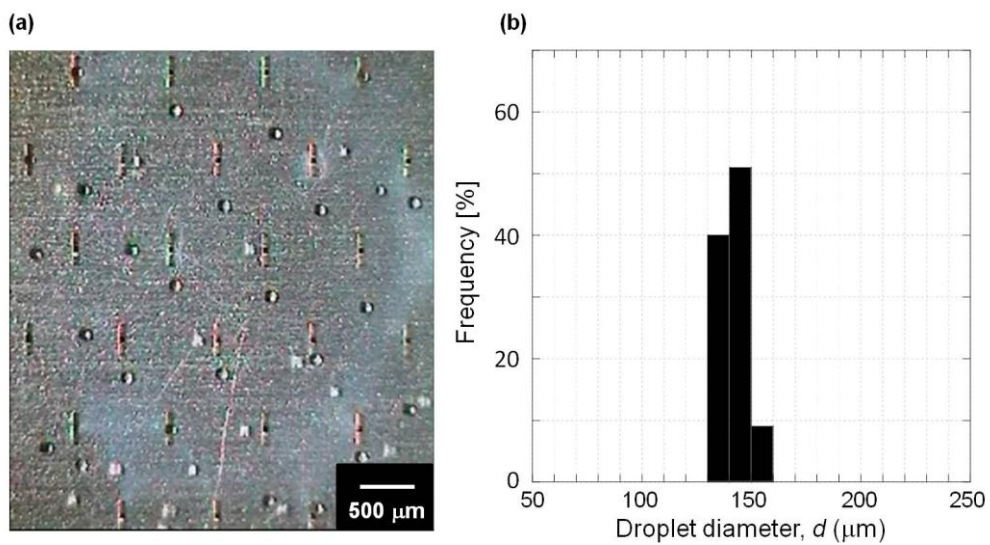
Figure 4-4 (a) Typical droplet generation results using WMS-Al-50 chips. (b) Size distributions of the oil droplets produced using WMS-Al-50.
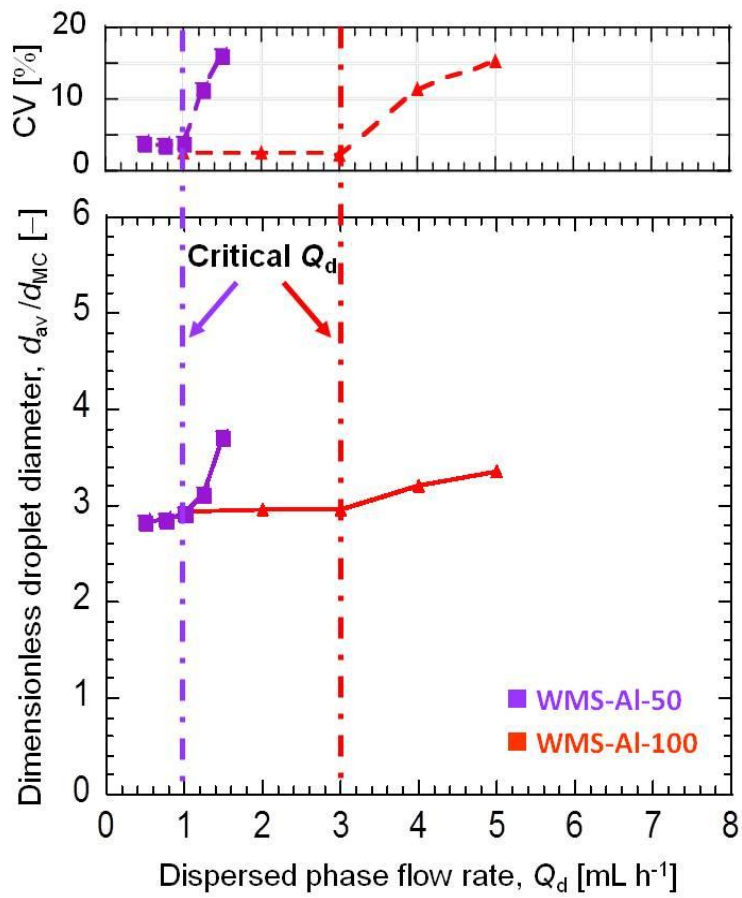
Figure 4-5 Effect of the flow rate of the dispersed phase (Q_d) on the average droplet diameter (d_{av}) and coefficient of variation (CV) obtained using a WMS-Al chip.

Thus, polydispersed emulsions were produced in the form of large droplets having broad size distributions with Q_d above the critical value., According to above results, the dispersed phase was found to be another important factor affecting the droplet size and size distribution when large droplets with diameter of >100 μm are generated at high Q_d.

4.3.3. Flow analysis of the dispersed and continuous phases using dimensionless numbers

The droplet generation behavior in MC emulsification is affected by flow rate of the dispersed phase and is dominated by the balance between interfacial tension and viscous force [13]. This balance is indicated by capillary number (Ca_d) and is expressed as:

$$Ca_d = \frac{\eta_d U_{d,MH}}{\gamma} \tag{3}$$

where η_d is the viscosity of the dispersed phase, γ is the interfacial tension between the dispersed and continuous phases, and $U_{d,MH}$ is the flow velocity of the dispersed phase in a circular microhole which is calculated by:

$$U_{d,MH} = \frac{\left(\left(\frac{\pi}{6} d_{av}^3\right) f_{MH}\right)}{A_{MH}} \tag{4}$$

where f_{MH} is the droplet generation frequency from the microhole and A_{MH} is the cross-sectional area of the microhole. f_{MH} was calculated by averaging the number of the droplets generated per second from a microhole. The $U_{d,MH}$ values at critical Q_d were 4.7 mm s^{-1} for WMS-Al-50 and 3.5 mm s^{-1} for WMS-Al-100. These critical $U_{d,MH}$ values are similar to those obtained by CFD simulation [15]. The previous CFD study considered the generation of a soybean oil droplet through an asymmetric MC into a water phase.
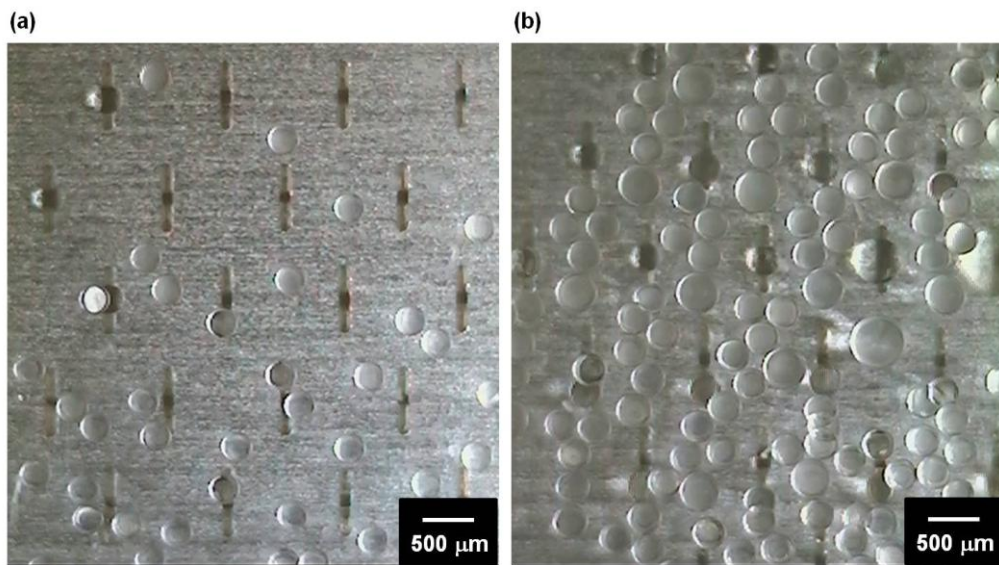
Figure 4-6 (a and b) Effect of Q_d on droplet generation (a) Typical droplet generation results under the critical Q_d, (b) Typical droplet generation results above the critical Q_d.

Fig. 4-7 represents the relationship between Ca_d and $\bar{d}$. The critical Ca_d was 0.045 for WMS-Al-50 and 0.034 for WMS-Al-100. Similar critical Ca_d values were reported for the generation of oil droplets with d_{av} of about 30 µm using a silicon MC array chip [15]. As shown in Fig. 4-7, $\bar{d}$ was almost constant below the critical Ca_d and sensitively varied above the critical Ca_d. Interfacial tension force dominates droplet generation below the critical Ca_d, leading to successful generation of uniform-sized droplets based on spontaneous transformation of the oil-water interface over the microhole outlet. In contrast, the viscous force reaches unignorable level above the critical Ca_d, so that resulting in the generation of nonuniform-sized droplets [18, 23]. The critical Ca_d for WMS-Al-50 was 1.3 times greater than that for WMS-Al-100. This difference is much smaller than the difference in the critical Q_d values (Fig. 4-5).

The flow state of the cross-flowing continuous phase was also investigated using a dimensionless number. The average velocity of the cross-flowing continuous phase ($U_{c,av}$) was calculated by

$$U_{c,av} = Q_c/A_{ch} \tag{5}$$

where A_{ch} is the cross-sectional area of the flow channel. $U_{c,av}$ values for WMS-Al-50 and WMS-Al-100 were 5.7 mm s^{-1} and 1.4 mms^{-1}, respectively. Next, the Reynolds number of the cross-flowing continuous phase (Re_c) was determined as

$$Re_c = \rho_c U_{c,av} d_{eq,ch}/\eta_c = \rho_c U_c(4A_{ch}/L_{ch})/\eta_c \tag{6}$$

where ρ_c is the continuous phase density, $d_{eq,ch}$ is the equivalent diameter of the flow channel, L_{ch} is the wetted perimeter of the flow channel, and η_c is the continuous phase viscosity. The Re_c values for WMS-Al-50 and WMS-Al-100 were 2.6 and 1.3, respectively, showing that the cross-flowing continuous phase applied in this study was
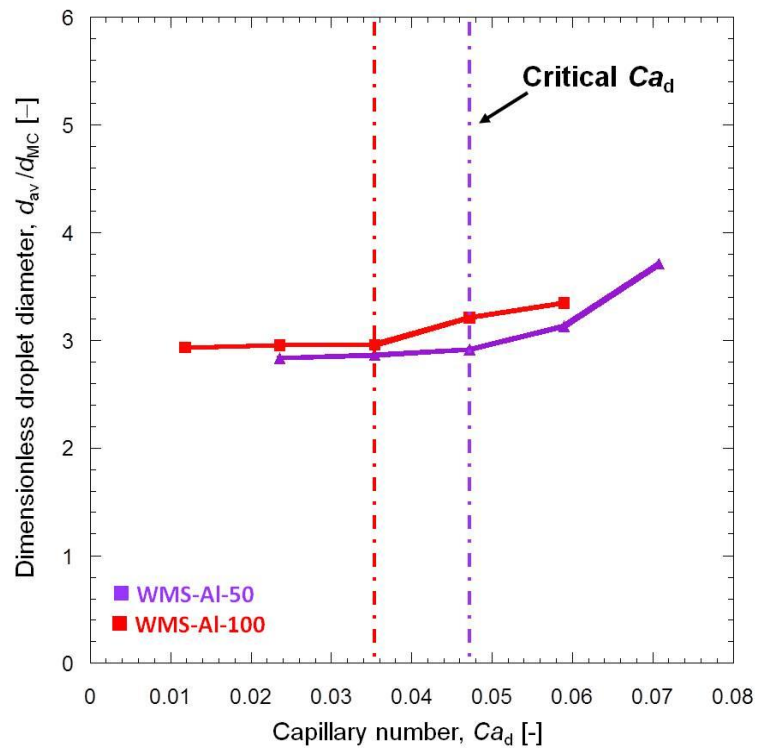
Figure 4-7 Variation of the dimensionless droplet diameter at different MC diameters as a function of the capillary number of the dispersed phase.

in a laminar state.

4.3.4. Force balance during droplet generation

Local continuous phase velocity affects the magnitude of drag force caused by the cross-flowing continuous phase (F_D). As we verified above, the continuous phase that flows in a laminar state in the channel has a parabolic velocity distribution. The continuous phase velocity has a maximum value at the center of a channel while it has a minimum value near the channel wall. The ratio of $U_{c,av}$ to the maximum continuous phase velocity ($U_{c,max}$) is speculated to be approximately 0.5 in a laminar state. For the expanding droplets, the continuous phase velocity at the center of the expanding droplets ($U_{c,dr}$) was given by

$$U_{c,dr} = U_{c,max}[1 - ((h_{c,ch} - d_{av})/h_{c,ch})^2] \qquad (7)$$

where $h_{c,ch}$ is the channel height. The droplet generation characteristics were influenced by the cross-flowing continuous phase exactly before the completion of droplet generation. At that moment, F_D can be obtained by the following equation:

$$F_D = 3k_x\pi\eta_c d_{av}U_{c,dr}[(1 + (2/3)\kappa)/(1 + \kappa)] \qquad (8)$$

where k_x (wall-correction factor for a sphere) is 1.7, and κ is the viscosity ratio of the continuous phase to the dispersed phase. F_D was considered as one of the promoting forces that induce droplet detachment from the slot outlet. The effect of Q_d and the type of MC array on F_D is plotted in Fig. 4-8. The F_D value hardly varied below the critical Q_d for both the WMS-Al chips. However, above the critical Q_d, the F_D value increased gradually with increasing Q_d for WMS-Al-50 and increased slightly with increasing Q_d for WMS-Al-100.

The variations of droplet diameter above the critical U_d is also related to the balance

82

of buoyancy force (F_B), inertial force (F_I), viscous force (F_V), and interfacial tension

force (F_γ), which acts on an expanding dispersed phase droplet (Figure 4-6b). These

forces are expressed by the following equations, respectively:

$$F_B = (\pi/6)d^3_{dr}g\Delta\rho \tag{7}$$

$$F_I = (\pi/3)\rho_d d_{MH}^2 U_d^2 \tag{8}$$

$$F_V = \mu_d d_{MH} U_d \tag{9}$$

$$F_\gamma = \pi d_{MH}\gamma \tag{10}$$

where g is the acceleration due to gravity, $\Delta\rho$ is the density difference between the two

phases, and ρ_d is dispersed phase density. Droplet generation is promoted by F_B, F_V, and

F_I but is restricted by $F\gamma$ at the neck. The values of F_B, F_V, and F_I and F_γ above or below

critical Q_d were respectively estimated using the preceding equations. The calculated

values of F_B, F_D and F_γ were plotted in Fig. 4-9. Both values of F_I and F_V had negligibly

small values ($<10^{-x}$), so that these two detachment-promoting forces need not be

considered. In contrast, F_γ had the highest value among these forces, indicating that

F_γ was the most important force acting on the expanding droplet. The F_γ values for the

WMS-Al chips were only affected by the d_{MH}. F_B was slightly depended on Q_d because

of the variation in the d_{av} (i.e, the d_{MH}). F_B was at least one order of magnitude smaller

than F_D but increased steeper than that of F_D with increasing Q_d. The F_D/F_B ratio

between F_D and F_B reduced from 63.8 to 47.6 for WMS-Al-50 and from 14.2 to 12.1 for

WMS-Al-100. The F_D/F_B ratio at critical Q_d was 62.0 for WMS-Al-50 and 14.0 for

WMS-Al-100. The confrontation between F_D and F_B certified that F_D is the second

important force in this study and that with the increasing d_{av} F_B became more effective

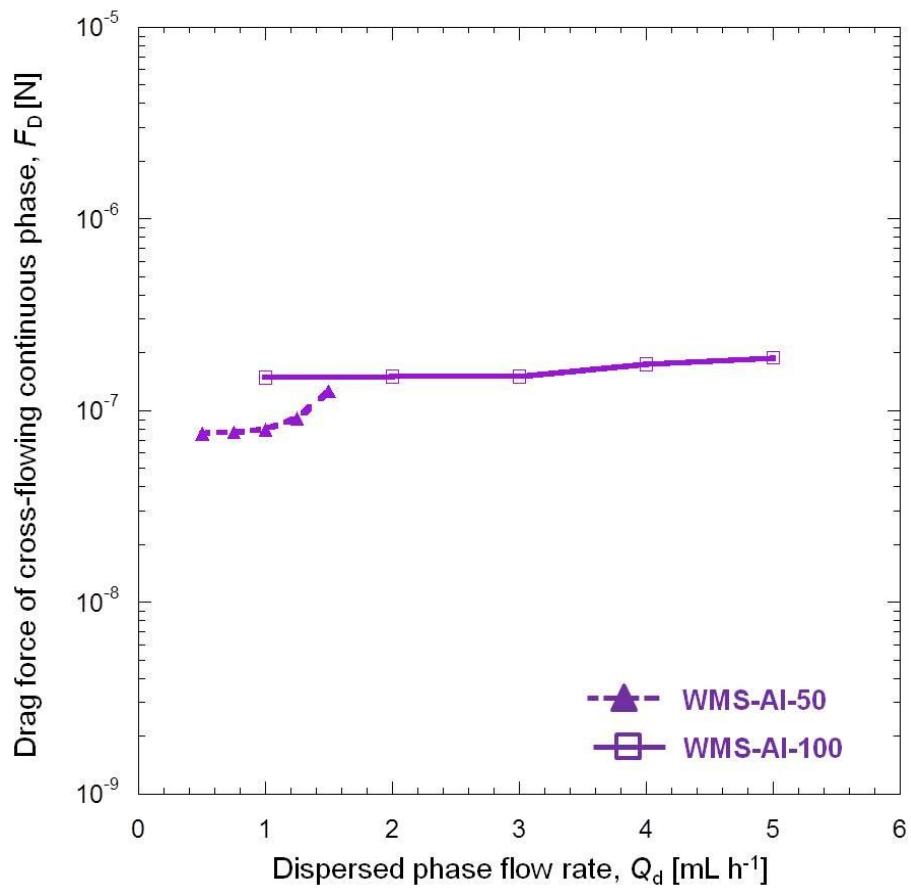force that acts on the expanding droplets. The value of F_γ was one order of magnitude

Figure 4-8 Effect of the flow rate of the dispersed phase (Q_d) on the drag force caused by a cross-flowing continuous phase (F_D).

greater than that of F_D. In spite of F_γ being more effective on the expanding droplets, F_D and F_B must be considered for droplet generation via large channels, as these forces were relatively greater orders of magnitude. We assume that the promotion forces contribute to the lower variation in droplet size for larger microholes at U_d above the critical value.

The analysis of the flow state of droplet generation using a dimensionless number (Ca_d) explain clearly the difference of the throughput capacities of monodisperse emulsion droplets between using the WMS-Al-50 and WMS-Al-100 in Tween 20 containing system, and the flow transition of the dispersed phase near the critical $U_{d,MC}$ was influenced by the balance between interfacial tension, buoyancy and drag forces, regardless of the diameter of circular MC.
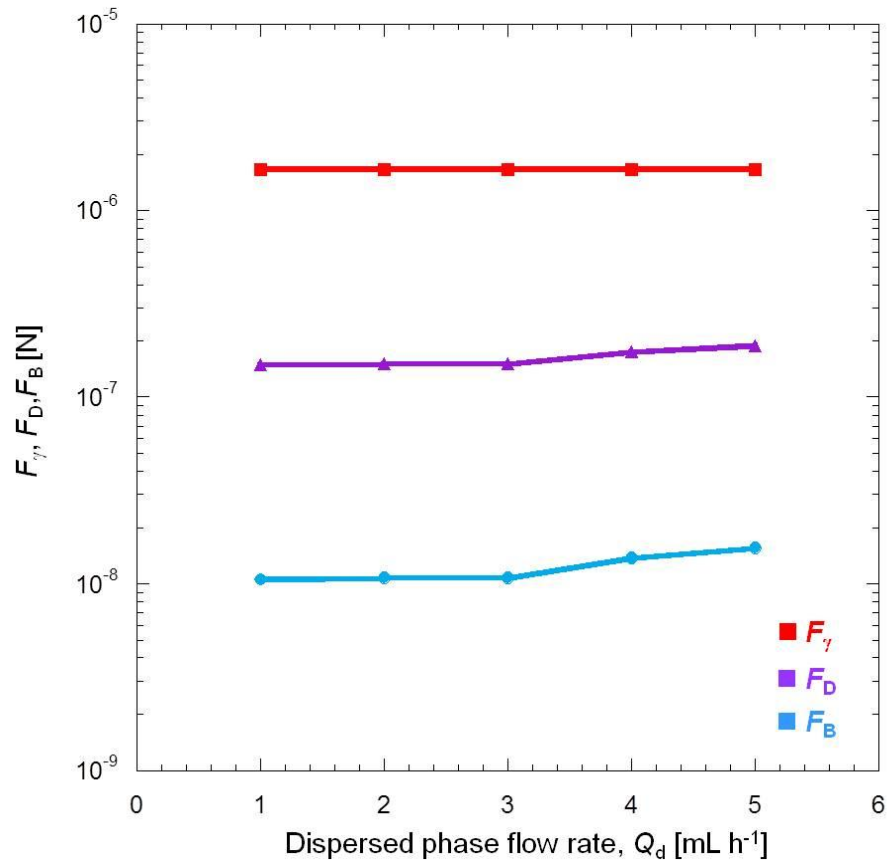
Figure 4-9 Effect of Q_d on the F_D, buoyancy force (F_B) and interfacial tension force (F_γ).

4.4. Conclusions

Metallic asymmetric straight-through MC array chips made of aluminum were successfully manufactured with precisely fabricated circular MC and micro-slot with d_{MC} of 50 or 100 μm. Uniform oil droplets with d_{av} proportional to d_{MC} were produced with CVs of less than 5%. The results obtained in this study also clarified the effect of Q_d on the droplet size, especially for such large droplets with sizes exceeding 100 μm. The resultant droplet size and size distribution was nearly independent of Q_d below the critical value, regardless of d_{MC}. In contrast, droplet size and its size distribution was highly dependent on Q_d above the critical value. The flow state of the dispersed phase during droplet generation via an aluminum asymmetric straight-through MC array could be characterized by Ca_d and the force balancing the droplet generation process. The results indicated that the drag forces (F_B, F_D) and the interfacial tension force (F_γ) become effective for droplet detachment above the critical U_d. These findings are expected to provide useful information on the generalized use of MC emulsification.

Chapter 5

General discussion

5.1. Introduction

In this chapter, I want to make a comparison of droplet generation charteristics of different material of MC plate. From this chapter we hope that we could make a discussion of such materials applied on MC plate fabrication and give some useful imformation for people to chosen a suitable material for their MC emulsification.

5.2 Droplet generation via asymmetric straight-through MC arrays made of different materials.

A previous study using WMS3-4 plate which has a circular MC diameter of 50um was same to the aluminum MC plate we developed. From fig. 5-1, we can clearly see that monodispersed oil droplets were stably generated via MC arrays using asymmetric silicon straight through MC arrays (WMS3-4).

However, in the case of the asymmetric straight-through MC array chip made by stainless-steel (WMS-SUS), the oil droplet detachment was unstable and the most number of microslot outlets were wetted by refined soybean oil act as the dispersed phase, only few number of uniform sized oil droplets generated from several microslots, regardless of the emulsifier types (Fig.5-2a). To successful produce uniform sized droplets, we chose another dispersed phase, silicone oil which has better hydrophobicity than that of soybean oil. The MC emulsification carried out with same Q_d and Q_c value that in the case of WMS-Al, and a Milli-Q water solution of 1.0 wt% Tween20 system was used as continuous phase. As presented in Fig. 5-2b, the disperse phase expanded rapidly from the microslot and form uniform sized oil droplet smoothly. This drop
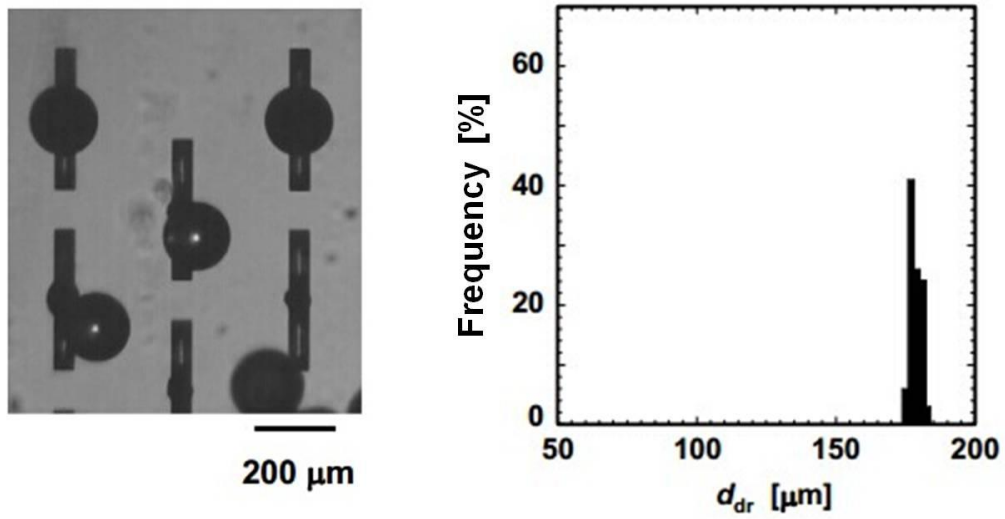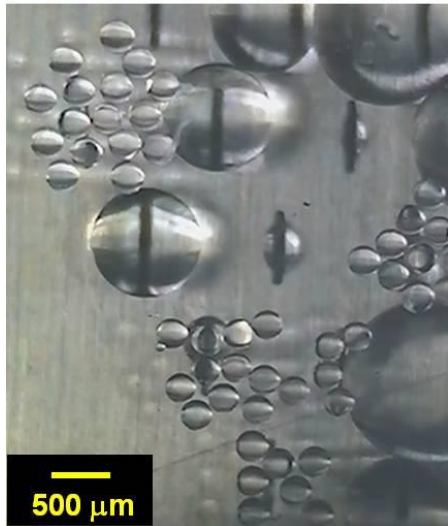
Figure 5-1. Typical droplet generation results using WMS3-4 chips. (b) Size distributions of the oil droplets produced using WMS3-4. (Kobayashi et al.,)

generation process occurred periodically from beginning to end of the whole MC emulsification process demonstrated that this system for WMS-SUS was capable of producing successful droplet generation. The resultant oil drops had a d_{av} of about 283.3 μm and CV below 4%. The successful droplets generation using silicone oil via WMS-SUS can be explained as follow. The type of silicon oil we use in this study is the most common one of dimethyl silicone oil, as the side chains of polysiloxane are entire of methyl group, this kind of oil have very good potential of water repellency. It means that the use of silicone oil as the dispersed phase was difficult wetted by the stainless-steel chip surface leads to a smooth detachment from the slot outlets of stainless-steel asymmetric straight-through MC array chip. The results obtained above clarified that WMS-SUS had less potential for monodispersed O/W emulsion generation as it has some limitation of dispersed phase selection. To explain the reason of this result, we also measured the static oil contact angle on the surface of two metal MC plates. From the previous study, we have knowledge that if the oil contact angle on the surface of the MC plate over critical value of 120 degree, smoothly droplet generation can be observed. In our case, the static oil contact angle on the surface of WMS-Al was more than 120° (Fig5-3a), which make it enable to produce monodispersed droplets stable. In the contrast, the contact angle on surface of WMS-SUS was less than the critical value that caused unstable droplet generation. In the other hand, when we change the oil to silicone oil to measure the static contact angle attached to stainless-steel MC plate, the results was quite higher than the critical value which can give a proof for contact angle measurement was one method for evaluate the droplet generation performance for different material of MC array plate (Fig5-3d).
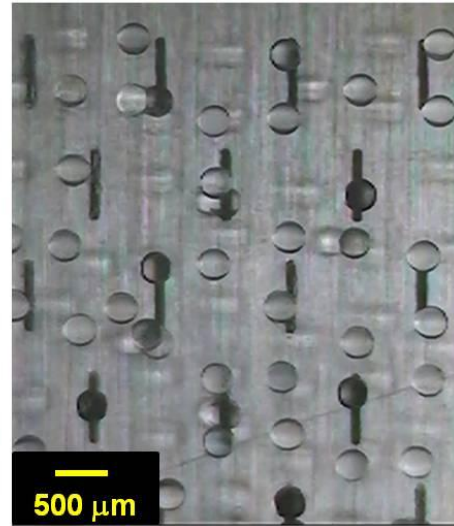
(a)   (b)

Soybean oil   **Silicone oil**
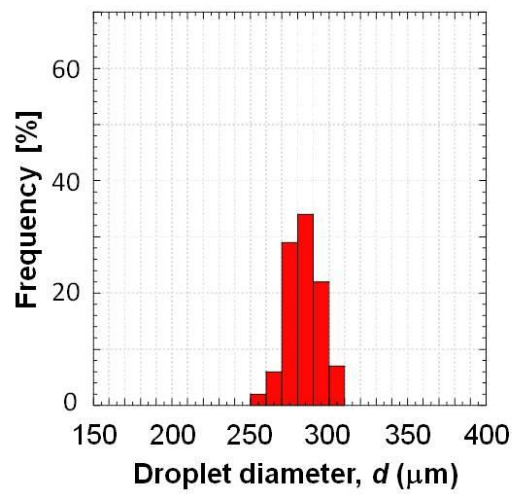
500 μm   500 μm

(c)

Figure 5-2 Typical droplet generation results using WMS-SUS-100 chips by using different dispersed phase. (a) Soybean oil. (b) Silicone oil. (c). Size distributions of the oil droplets produced by WMS-SUS-100 using silicone oil as the dispersed phase.
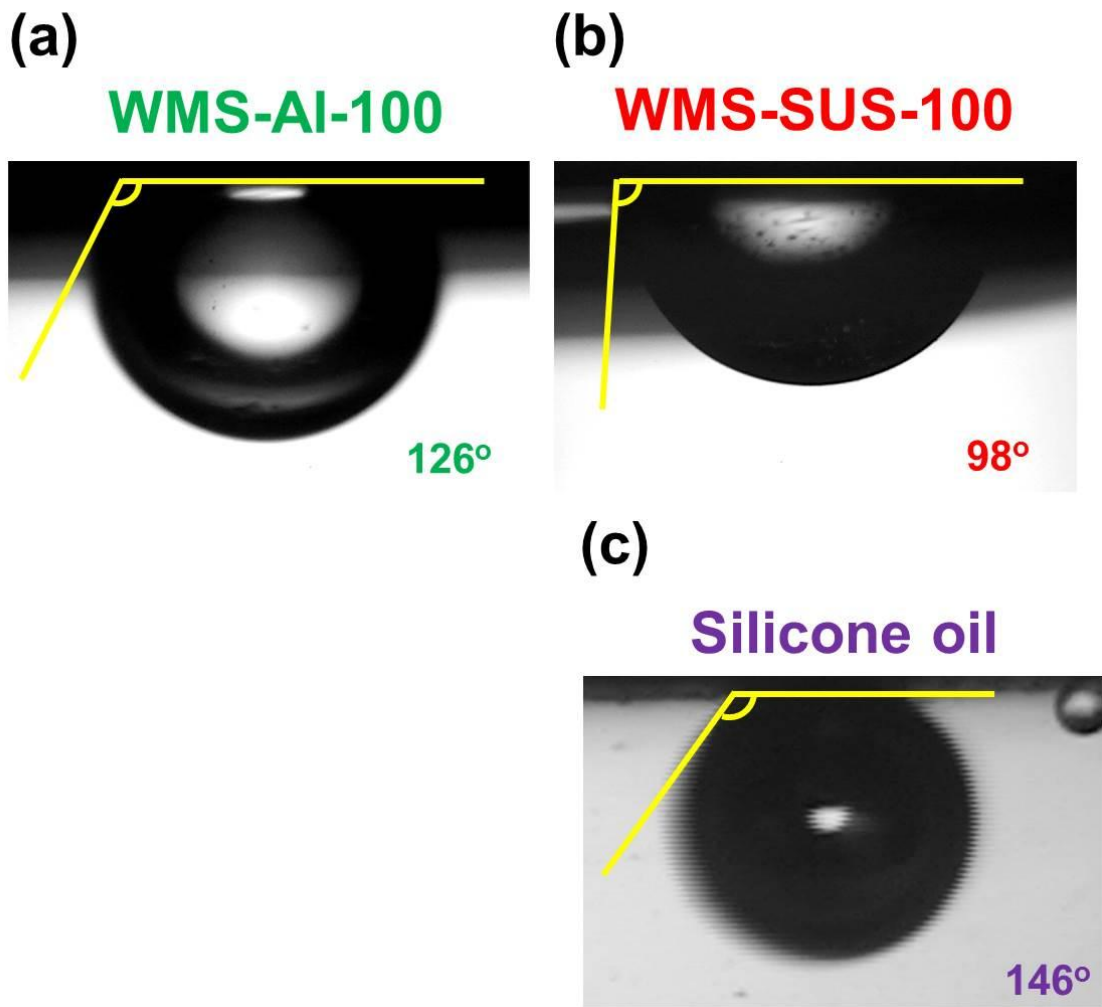
Figure 5-3 Typical images of oil drop on the different MC plate surfaces using different oils. (a)WMS-Al-100. (b)WMS-SUS-100 (Soybean oil). (c) WMS-SUS-100 (Silicone oil).

5.3 Effect of pH on O/W emulsion generation characteristic

Was investigated the effect of pH on O/W emulsion generation characteristic by using WMS-Al-100 in the same SDS containing system. At pH5, unstable droplet generation was observed, in the other hand, in a continuous phase at pH7, monodisperse oil droplet can be stably produced. From this result, we can say, preparation stability of O/W emulsion using WMS-Al-100 was dependent on the pH of the continuous phase. The reason of this result can be considered about the isoelectric point of the alumina is 7.4 to 9. The alumina surface of the aluminum chip could be considered be positively charged in an acidic environment. Therefore, since the affinity between the chip surface and the anionic emulsifier SDS, production of oil droplets is considered to become unstable.

We also investigate the effect of pH on O/W emulsion generation characteristic by using WMS-SUS-100. the result was quite different from that we got of using aluminum plate. In this case the droplet generation was independent on the pH of the continuous phase.

5.4 Comparison of silicon MC plates with metallic MC plates

Was concluded the physical properties and droplet generation performance of these three kinds of material of MC array plate. For the hydrophilicity of the MC plate surface, silicon MC plate has best performance, and both of silicon MC array plate and stainless-steel MC array plate have good anti- acid ability. In the case of anti-alkalis ability, stainless-steel have very good performance. Also for the shock proof ability both aluminum and stainless-steel MC array plate have better performance. From above physical properties, I considerate that silicon MC array plate even lack for some shock proof ability have better droplet generation performance. But for generic use of MC emulsification, we can choose the MC plate material case by case. And for better droplet generation performance of metallic MC array plate, we also need some information of suitable storage condition for maintain their hydrophilic plate surface.
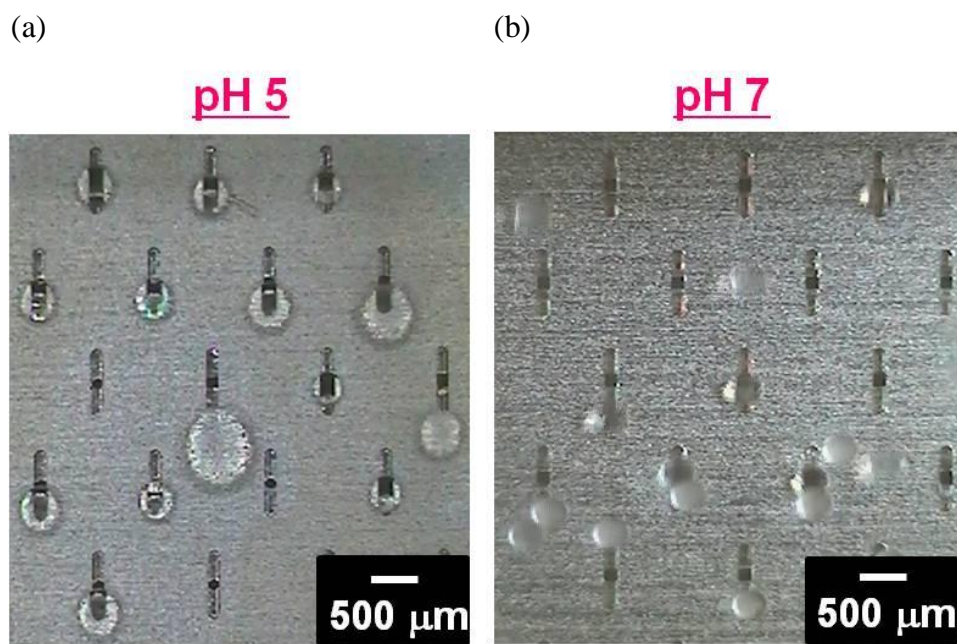
Figure 5-4 Effect of pH on O/W emulsion generation characteristic using WMS-Al-100.
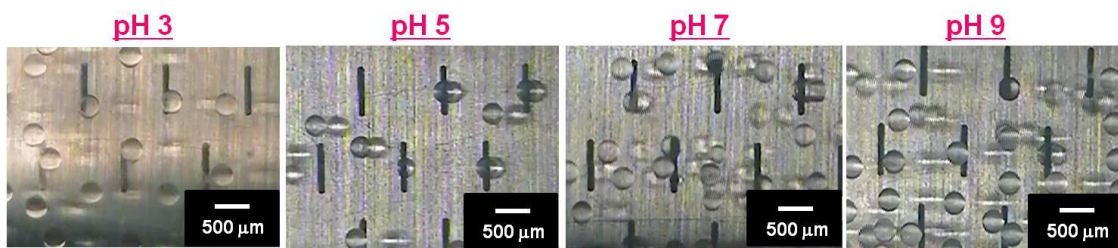
(a) pH 5. (b) pH 7.

Figure 5-5 Effect of pH on O/W emulsion generation characteristic using WMS-SUS-100.
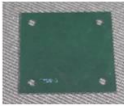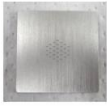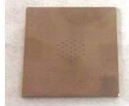
	Silicon MC array plate	Aluminum MC array plate	Stainless-steel MC array plate
Hydrophilicity	＋＋＋＋	＋＋	＋
Anti-acid ability	＋＋＋＋	＋	＋＋＋＋
Anti-alkalis ability	＋	＋＋	＋＋＋＋
Shock proof ability	＋	＋＋＋＋	＋＋＋＋
Droplet generation stability (O/W)	＋＋＋	＋＋	＋＋
Suitable emulsifier — Anionic	＋＋＋＋	＋＋＋	＋＋＋
Suitable emulsifier — Nonionic	＋＋＋	＋＋	＋＋
Suitable storage condition	Milli-Q water	Air?	Air?

Figure 5-6 Comparison of silicon MC plates with metallic MC plates.

Chapter 6

General Conclusions and Prospectives

6.1 Introduction

This study focuses on several issues related to MC emulsification, especially for the assessment for stable and practical scale production of MC emulsification and assessment for generic use of MC emulsification. In MC emulsification, the dispersed phase contact angle to the MC plate is a key parameter affecting droplet generation from the channels, since the production of O/W emulsions need a sufficiently hydrophilic MC plate surface. Optimization of storage conditions of the MC plate is important to maintain the hydrophilic surface properties of MC plate much longer. The effects of storage conditions, temperature, pH and storage period on the water contact angle to the MC plate were analyzed respectively. In addition, stably continuous MC emulsification is needed for bulk production on both lab and industry scales. Droplet size, droplet size distribution, and droplet generation during continues MC emulsification up to one week were analyzed by using different emulsifiers. The need for generic use of metallic MC arrays with mass production ability has been arising. Prior to developing large scale metallic MC arrays, the droplet generation characteristics of metallic asymmetric straight-through MC array chip have been investigated. Thus, an aluminum asymmetric straight-through MC array chips, each of them consisting of a precisely microfabricated asymmetric straight-through geometry in one plate, were developed. The characteristics of droplet generation, size and size distribution of the generated oil droplets and the effect of dispersed phase flow rate on droplet generation were investigated. The dispersed phase flow during droplet generation was also analyzed using dimensionless number.

6.2 Summary of each chapter

Chapter 1

Fundamentals of emulsion, microfabrication technology, microfabrication process, continuous emulsification and contact angle were reviewed. Emulsion principles, properties characterization, types, fundamentals, and applications of emulsification devices were defined. The objectives of this thesis were described.

Chapter 2

MC emulsification is a promising technique to produce monodisperse emulsions by spontaneous interfacial-tension-driven droplet generation. This study characterized the effect of storage conditions on the water contact angle to the silicon MC plate, which is an uncharted area. The silicon MC plate surfaces were treated with oxygen plasma for 1 to 60 min. Following to that, each silicon plate was stored in air, 0.1 mol/L nitric acid, or Milli-Q water at different temperatures. The change in the hydrophilicity of the MC plate surface was monitored with contact angle measurement. The oxygen plasma treatment caused a remarkable decrease in the water contact angle on the plate surface from 84° to 8°. The treatment time had a negligible effect on the water contact angle value. However, the plate surface gradually lost its hydrophilicity expressed as the water contact angle with time. The rate of this process was influenced by both storage medium and temperature. During 10 days of storage, the MC plates stored in water had the lowest water contact angles, and those stored in air had the highest water contact angle. The reason for decreasing hydrophilicity of the MC plates can be explained as follows. Air is a hydrophobic fluid. Although nitric acid is a hydrophilic fluid, nitric acid molecules were dissociated into nitrate and hydrogen ions. The interaction between

positively charged hydrogen ions and negatively charged silanol group formed on the plate surface affects the decreasing hydrophilicity of the MC plates. The preparation characteristics of O/W emulsification using two emulsifiers by using different surface conditioned MC plate were analyzed. Droplet generation was carried out by using a silicon MC plate (MSX11) just after oxygen plasma treatment, the MC plate stored in air at 50°C, and the MC plate stored for >1 year. Tween 20 and SDS were used as emulsifiers. The zeta potential of MC plate surface soaked in Tween 20 was -85.0 mV. In contrast, the zeta potential of MC plate surface soaked in SDS was highly negative charged with a value of -200 mV. When a nonionic emulsifier (Tween 20) was used, the advancing contact angle of the dispersed phase of the MC plate stored for >1 year was much higher than its receding contact angle. The use of this MC plate resulted in producing polydisperse soybean oil droplets with a CV over 20%. The advancing contact angle of the dispersed phase to the MC plate just after oxygen plasma treatment was similar to its receding contact angle. By contrast, monodisperse oil droplets with CV below 3% were obtained using this MC plate. In addition, when an anionic emulsifier (SDS) was used, the advancing contact angle of the dispersed phase of the MC plate stored for >1 year was similar to its receding contact angle. Relatively polydisperse oil droplets with CV of about 9% were obtained using this MC plate.

Chapter 3

The preparation characteristics of O/W emulsions during continuous MC emulsifications were investigated. Tween 20 and SDS were used as emulsifiers. During 7 days storage in the dispersed phase that imitates continuous MC emulsification, the water contact angle to the MC plate remained $<30^{o}$. For the Tween 20-containing

system, the average diameter of the generated oil droplets slightly increased with time, and their CV gradually increased with time. For the SDS-containing system, monodisperse oil droplets with CV below 5% were obtained during of the entire continuous MC emulsification, with a negligible change of their average diameter caused by strong repulsive force between the dispersed phase covered by negatively charged anionic emulsifier (SDS) and the negatively charged silanol group formed on the MC plate surface.

Chapter 4

In this chapter, we investigated the production characteristics of monodisperse oil-in-water (O/W) emulsions formulated by using newly designed asymmetric straight-through MC arrays made of aluminum. These aluminum MC arrays were fabricated through microdrilling process with a diameter of 50 or 100 μm, while microslots were fabricated through electric discharge machining. Refined soybean oil was used as the dispersed phase and 1 wt% Tween 20 in Milli-Q water as the continuous phase. The metallic MCs with 100 μm diameter produced monodisperse O/W emulsion droplets with average diameters (d_{av}) of about 300 µm and coefficients of variation (CVs) below 4%. Meanwhile, the metallic MC array with 50 μm diameter stably generate monodisperse O/W emulsion droplets with d_{av} of about 150 μm and CV below 4%. The d_{av} of the generated oil droplets was nearly proportional to the MC diameter. Monodisperse O/W emulsions were also successfully generated below the critical flow rate of the dispersed phase, with little variation in d_{av} and CV values.

Chapter 5

Monodisperse O/W emulsions can be stable generated using asymmetric straight-through MC arrays made by different material. The droplet generation characteristic can be explained by contact angle measurement. Preparation stability of O/W emulsion using WMS-Al-100 was dependent on the pH of the continuous phase. In the other hand, preparation stability of oil droplets generation by WMS-SUS-100 was independent on the pH of the continuous phase. Each MC arrays has their own advantages and disadvantages, material chosen should be talked case by case (e.g. an anionic emulsifier have best combination with silicon based MC plate).

6.3 General conclusions

◆ The single-crystal silicon MC plate used in this study was effectively converted into a high hydrophilicity by oxygen plasma treatment.

◆ The hydrophilicity of MC plate surface was best maintained in Milli-Q water at low temperature.

◆ Our results clarified that the hydrophilic property of the plasma treated MC plate was better kept by storing in a hydrophilic medium with a low concentration of positively charged hydrogen ions which have affinity with negatively charged MC plate surface and with a highly negative charge zeta potential.

◆ This study elucidates that monodispersed droplets could not be produced when using a MC plate on air stored for >1 year, regardless of using nonionic or anionic emulsifier.

◆ The continuous MC emulsification results clarified that anionic emulsifier had good potential for continuous MC emulsification.

- Our results clarified that both of aluminum or stainless-steel asymmetric straight-through microchannel arrays were capable of producing monodisperse O/W emulsions by using different oil.

- The findings of metallic asymmetric straight-through MC array expected to provide useful information on the generalized use of MC emulsification.

- This study shown that different kinds of materials for fabricating MC arrays has their own advantages and disadvantages, material chosen should be talked respectively.

6.4 Prospectives

Emulsification with microfabriceted devices have been investigated during the last twenty years, many developments in this subject had occurred recently. It is highly expected that this technology will become available for large scale production of monodisperse single and double emulsions. The strong interest of various industries and academic groups in producing monodispersed droplets in a mild way, lead us to believe that a scaled-up processes is relevant. The author expects that MC emulsification devices will be scaled up, the stable continuous emulsification could be used for better productivity. The author expects the future application of MC emulsification in the industry, in the production of food emulsions with large throughputs and focus on monodispersity and bulk production for the pharmaceutical industry.

The research finding in this thesis could also have future applications in the storage method of MC plate that could keep surface hydrophilicity in a relatively long time and an anionic emulsifier used for continuous MC emulsification. Moreover, the metallic MC plate may achieve generic use of MC emulsification. Further study on MC plate

storage conditions which has less oxygen effect or with a low concentration of hydrogen ions need to be investigated. Moreover further investigation is needed in surface properties of MC plate from a microcosmic view. To understand the interaction between different material of MC plate surface and storage conditions occurred in a microcosmic way is important. In addition, anionic emulsifier for non-food use was depicted with good potential to stabilize continuous MC emulsification, so it is important to understand droplet generation behavior during continuous MC emulsification by using some food grade emulsifiers and food grade materials, which could have a good application on continuous production of high-value added food emulsions. It was expected that the results obtained in this thesis could have some useful information for mass production and generic use of MC emulsification.

Literatures Cited

Abrahamsw A J, van Lierop R, van der Sam RGM, van der Padt A, Boom R M (2002) Analysis of droplet formation and interactions during cross-flow membrane emulsification. J Membrane Sci 204:125-137

Anna S L, Bontoux N, and Stone H A (2003) Formation of dispersions using flow-focusing in microchannels. Appl Phys Lett 82:364-366

Anna S L, Bonyoux N, Stone H A (2003) Formation of dispersions using "flow focusing" in microchannels. Appl Phys Lett 82:364-366

Altenbach-Rehm J, Suzuki K, Schubert H, Production of o/w-emulsions with narrow droplet size distribution by repeated premix membrane emulsification, 3ieme Congres Mondial de l'Emulsion, 24-27 September 2002, Lyon, France.

Ax K, Mayer-Miebach E, Link B, Schuchmann H, Schubert H (2003) Stability of lycopene in oil-in-water emulsions. Eng Life Sci 3:199-201

Bibette J (1991) Depletion interactions and fractionated crystallizationfor polydisperse emulsion purification. J Colloid Interface Sci 147:474-478

Brouzes D, Medkova M, Saveneli N, Marran D, Twardowski M, Hutchison J B, Rothberg J M, Link D R, Perrimon N, Samuels M (2009) Droplet microfluidic technology for single-cell high-throughput screening. PNAS 106:14195-14200

Charcosset C (2009) A review of membrane processed and renewable energies for desalination. Engineering with Membrane 245:214-231

Chen I J and Lindner E. (2007) The stability of Radio-Frequency plasma-treated polydimethylsiloxane surfaces. American Chemical Society. 23: 3118-3122

Chuah A M, Kuroiwa T, Kobayashi I, Zhang X, Nakajima M (2010) Preparation of

uniformly sized alginate microspheres using the novel combined methods of microchannel emulsification and external gelation. Colloids Furf A 351:9-17

Chu L Y, Park S H, Yamaguchi T, Nakao S (2011) Preparation of thermo-responsive core-shell microcapsules with a porus membrane and poly (N-isopropylacrulamide). J Membr Sci 192:27-39

Comiskey B, Albert J D, Yoshizawa H, Jacobson J (1998) An eletrophoretic ink for all-printed reflective electronic displays. Nature 394:253-255

De Geest B G, Urbanski J P, Thorsen T, Demeester J, De smedt SC (2005) Synthesis of monodisperse biodegradable microgels in microfluidic devices. Langmuir 21:10275-10279

Dendukuri D, Tsoi K, Hatton T A, Doyle P S (2005) Controlled synthesis of nonspherical microparticles using microfluidics. Langmuir 21: 2113-2116

Dickinson E (1992) Introduction to Food Colloids, Oxford University Press, Oxford, UK.

Dowding P J, Goodwin J W, Vincent B (2001) Production of porous suspension polymer bean with a narrow size distribution using a cross-flow membrane and a continuous tubular reactor. Coll Sur. A 180:301-309

Ehrfeld W, Golbig K, Hessel V, Lowe H, Richter T (1999) Characterization of mixing in micromixers by a test reaction, single mixing unit and mixers arrays. Ind Eng Chem Res 38:1075-1082.

Ehrfeld W, Hessel V, Lowe H (2000) Microreactors. VCH, Weinheim p.70

Evans D F and Wennerstrom H (1994) The Colloidal Domain: Where Physics, Chemistry, Biology and Technology Meet. VCH Publishers New York.

Geerken M J, Lammertink RGH, Wessling M (2007) Interfacial aspects of water drop

formation at micro-engineered orifices. J Colloid Interface Sci 312:460-469

Gijsbertsen-Abrahamse A J (2003) Membrane Emulsification: Process Principles. PhD Thesis Wageningen University

Gu Y, Li D (2000) The ζ-Potential of glass surface in contact with aqueous solutions. J colloid Interface Sci 226:328-339.

Hardt S, Schonfeld F, Weise F, Hoffmann C, Hessel V, Ehrfeld W (2001) ProReferences 171 ceedings of the 4th International Conference on Modeling and Simulations of Microsystems 2011, Hilton Head Island, SC, pp:233-226

Harvkamp V, Ehrfeld W, Gebauer K, Hessel V, Lowe H, Richter T, Wille C (1999) The potential of micromixers for contacting of disperse liquid phases Fresenius. J Anal Chem 364: 617-624.

Hatate Y, Uemura Y, Ijichi K, Kato Y, Hano T (1995) Preparation of GPC packed beads by a SPG membrane emulsifier, J Chem Eng Japan 28: 656-659

Herweck T, Hardt S, Hessel V, Löwe H, Hoffmann C, Weise F, Dietrich T, Freitag A, Miccroreaction Technology (Proceedings of the Fifth International Conference on Microreactin Technology), Springer, Berlin, Germany, 2001, pp. 216-229

Hunter R J (1986) Foundations of Colloid Sciences. Vol 1 Oxford University Press, Oxford pp 752

Israelachvili J J (1992) Intermolecular and surface forces. Academic press. London, UK.

Iwamoto S, Nakagawa K, Sugiura S, Nakajima M (2002) Preparation of gelatin microbeads with a narrow size distribution using microchannel emulsification. AAPS Pharm Sci Tech 3: 72-76

Joscelyne S, and Trägårdh G (2000) Membrane emulsification – A literature review. J

Membrane Sci 169:107-117

Kawakatsu T, Kikuchi Y, Nakajima M (1997) Regular sized cell creation in microchannel emulsification by visual microprocessing method. J Am Oil Chem Soc 74:317-321

Kawakatsu T, Oda N, Yonemoto T, Nakajima M (1999) Production of monodispersed albumin gel microcapsules using microchannel W/O emulsification. Kagaku Kogaku Ronbun 26:122-125

Kawakatsu T, Trägårdh G, Trägårdh Ch (2001) Production of W/O/W emulsions and S/O/W pectin microcapsules by microchannel emulsification. Colloid Surf A 189:257-264

Kikuchi Y, Sato K, Kaneko T (1992) Optically accessible microchannels formed in a single-crystal silicon substrate for studies of blood rheology, Microvase Res 4:226-240

Kobayashi I, Yasuno M, Iwamoto S, Shono A, Satoh K, Nakajima M (2002a) Microscopic observation of emulsion droplet formation from a polycarbonate membrane. Colloids Surf A 207:185-196

Kobayashi I, and Nakajima M (2002b) Effect of emulsifiers on the preparation of food-grade oil-in-water emulsions using a straight-through extrusion filter. Eur J Lipid Sci Technol 104:720-727

Kobayashi I, Nakajima M, Chun K, Kikuchi Y, Fujita H (2002c) Silicon array of elongated through-holes for monodisperse emulsion droplets. AIChE J 48:1639-1644

Kobayashi I, Nakajima M, Mukataka S (2003a) Preparation characteristic of oil-in-water emulsion using differently charged surfactants in straight-trough

microchannel emulsification Colloids Surf A 229: 33-41

Kobayashi I, Iitaka Y, Iwamoto S, Kimura S, Nakajima M, Mukataka S (2003b) Preparation characteristic of lipid microspheres using microchannel emulsification and solvent evaporation. J. Chem. Eng. Japan, 36: 996-1000

Kobayashi I, Mutakata S, Nakajima M (2005a) Novel asymmetric through-hole array microfabricated on a silicon plate for formulating monodisperse emulsions. Langmuir 21: 7629-7632

Kobayashi I, Lou X, Mutakata S and Nakajima M (2005b) Preparation of monodisperse water-in-oil-in-water multiple emulsion using microchannel emulsification. J Am Oil Chem Soc. 82: 65-71

Kobayashi I, Nakajima M (2006) Generation and multiphare flow of emulsions in microchannels. In Kockmann N (ed) Micro Process Engineering, Wiley-VCH, Werinheim

Kobayashi I, Uemura K, Nakajima M (2007) Formulation of monodisperse emulsions using submicron-channel arrays. Colloids Surf A 296:285-289

Kobayashi I, Takano T, Maeda R, Wada Y, Uemura K, Nakajima M (2008a) Straight-through microchannel devices for generating monodisperse emulsion droplets several microns in size. Microfluid Nanofluid 4:167-177

Kobayashi I, Hirose S, Katoh T, Zhang Y, Uemura K, Nakajima M (2008b) High-aspect-ratio through-role array microfabricated in PMMA plate for monodisperse emulsion production. Microsyst. Technol, 14:1379-1357

Kobayashi I, Hori Y, Uemura K, Nakajima M (2010) Production characteristics of large soybean oil droplet by microchannel emulsification using asymmetric through holes. Jpn J Food Eng 11:37-48

Köster S, Angilė F E, Duan H, Agresti JJ, Wintner A, Schmitz C, Rowat A C, Merten C A, Pisignano D, Groffiths A D, Weitz D A (2008) Drop-base microfluidic devices for encapsulation of single cells. Lab Chip 8:1110-1115

Butron F K, Kobayashi I, Uemura K, Nakajima M (2011) Temperature effect on microchannel oil-in-water emulsification. Microfluid Nanofluid 10:773-783

Butron F K, Kobayashi I, Neves M A, Uemura K, Nakajima M (2011) Effect of temperature on production of soybean oil-in-water emulsions by microchannel emulsification using different emulsions. Food Sci. Technol. Res. 17: 77-86

Link D R, Anna S L, Weitz D A, Stone HA (2004) Geometrically mediated breakup of drops in microfluidic devices. Phys Rev Lett 92: 054503-054507

Lucassen-Reynders E H, Kuijpers K A (1991) The Role of Interfacial properties in emulsification. Colloids Surf 65:175-184

Mason T G, Krall A H, Gang H, Bibette J and Weitz (1996a) Monodisperse Emulsions Properties and Used. In: Encyclopedia of Emulsion Technology (P. Becher ed.) vol 4, Marcel Dekker, New York, pp 299-335

Mason T G, Bitte J and Weitz D A (1996b) Yielding and flow of monodisperse emulsions (1996b) J Coll Interf Sci 179: 439-448

Mahajan R K, Chawla J, Bakshi M S, (2004) Depression in the cloud point of Tween in the presence of glycol additives and triblock polymers. Colloid Polym Sic 282:1165-1168

McClements D J (2004) Food Emulsions: Principles, Practice, and Techniques. 2nd Edition, CRC Press, Boca Raton

Murshed SMS, Tan SH, Nguyen NT, Wong TN, Yobas L (2008) Microdroplet formation

of water and nanofluids in heat-induced microfluidc T-junction. Microfluid Nanofluid 6:253-259

Myers D (1988). Surfactant Sci and Tech. 2nd Edition, VCH

Nagashima S, Ando S, Tsukamoto T, Ohshima H, Makino K (1998) Preparation of monodisperse poly(acrylamide-co-acrylic acid) hydrogel nicrospheres by membrane emulsification technique and their size-dependent surface properties. Colloid Surf B 11:27-56

Nakagawa K, Iwamoto S, Nakajima M, Shono A and Satoh K (2004) Microchannel emulsification using gelatin and surface-free coacervate microencapsulation. J Colloid Interface Sci 278:198-205

Nakashima T, Shimizu M and Kukizaki M (1991) Membrane emulsification by microporous glass. Key Eng Mater 61/62:513-516

Nakaya K, Kohata T, Doisaki N, Ushio H, Ohshima T. (2006) Effect of oil droplet sizes oil-in-water emulsion on the taste impressions of added tastants. J Phys Chem 72: 877-883

Neves M A, Ribeiro H S, Kobayashi I, Nakajima M (2008a) Encapsulation of lipopfilic bioactive molecules by microchannel emulsification. Food Biophysics 3:126-131

Neves M A, Ribeiro H S, Fujiu K B, Kobayashi I, Nakajima M (2008b) Formulation of controlled size PUFA-loaded oil-in-water emulsions by microchannel emulsification using β carotene-rich palm Ind Eng Chem Res, 47:6405-6411

Nguyen N T and Wereley S T (2002) Fundamentals and Applications of Microfluidics Artech House, Boston, USA, pp. 67-129

Nguyen N T, Ting T H, Yap Y F, Wong T N, Chai JCK (2007) Thermally mediated

droplet formation in microchannels. Appl Phys Lett 91:084102- 084102-3

Nishisako T, Torii T, Higuchi T (2004) Novel microreactor for functional polymer beads. Chem Eng J 101:23-29

Nishisako T, Torii T (2008) Microfluidic large-scale integration on a chip for mass production of monodisperse droplets and particles. Lab Chip 8:287-293

Okochi H, Nakano M (1997) Comparative study of two preparation method of w/o/w emulsions: stirring and membrane emulsification. Chem Pharm Bull 45:1323-1326

Okushima S, Niahisako T, Torri T, Higuchi T (2004) Controlled production of monodisperse double emulsions by two-step droplet breakup in microfluidic devices. Langmuir 20: 9905-9908

Opawale F, Burgess D (1998) Influence of interfacial properties of lipophilic surfactants on water-in-oil emulsion stability. J Colloid Interface Sci 197:142-150

Peng S J, Williams R A (1998) Controlled production of emulsions using a crossflow membrane. Part I: droplet formation from a single pore. Trans Inst Chem Eng 76:894-901

Ribeiro H S, Rico L G, Badolato G G, Schubert H (2005) Production of O/W emulsions containing astaxanthin by repeat premix membrane emulsification. J Food Sci 70: E117-E123

Ribeiro H S, Janssen J, Kobayashi I, Nakajima M (2010) Membrane Emulsification for Food Applications. Membrane Technology Membranes for Food Applications. Chapter 7:129-166. Wiley-VCH Verlag GmbH & Co. KGaA

Rosen M J (2004). Surfactants and interfacial phenomena. J Wiley and Sons. USA

Ruijter M, Kölsch P, Voué M, De Coninck J, Rabe J P (1998) Effect of temperature on

the dynamic contact angle. Colloids Surf 144:235-243

Schaerli Y, Hollfelder F (2009) The potential of microfluidic water-in-oil droplets in experimental biology. Molecular Biosystems 5: 1392-1404

Scherze I, Knöfel R, Muschiolik G (2005) Automated image analysis as a controltool for multiple emulsions. Food Hydrocoll 19: 617-624

Schröder V, Behrend O and Schubert H (1998) Effect of dynamic interfacial tension on the emulsification process using microporous ceramic membranes. J Colloid Interface Sci 202:334-340

Schröder V, Schubert H (1999) Production of emulsions using microporous ceramic membranes. Colloid Surf A 152: 103-109

Shiau B J, Sabatini D A, Harwell JYH (1995) Properties of food grade (edible) surfactants affectin subsurface remediation of chlorinated. Environ Sci Techno 29, 2929-2935

Stan C A, Tang SKY, Whitesides G M (2009) Independent control of drop size and velocity in microfluidic flow-flocusing fenerators using variable temperature and flow rate. Anal Chem 81: 2399-2402

Sugiura S, Nakajima M, Tong J, Nabetani H, Seki M (2000) Preparation of monodispersed solid lipid microspheres using microchannel emulsification technique. J Colloid Interface Sci 227: 95-103

Sugiura S, Nakajima M, Ushijima H, Yamamoto K, Seki M (2001a) Preparation characteristics of monodispersed water-in-oil emulsions using microchannel emulsification. J Chem Eng of Japan 34:757-765

Sugiura S, Nakajima M, Iwamoto S, Seki M (2001b) Interfacial tension driven monodispersed droplet formation from microfabricated channel array.

Langmuir 17: 5562-5566

Sugiura S, Nakajima M, Kumazawa N, Iwamoto S, Seki M (2002a) Characterization of spontaneous transformation-based droplet formation during microchannel emulsification. J Phys Chem B 106: 9405-9409

Sugiura S, Nakajima M, Seki M (2002b) Effect of channel structure on microchannel emulsification. Langmuir 18: 5708-5712

Sugiura S, Nakajima M, Yamamoto K, Iwamoto S, Oda T, Satake M, Seki M (2004a) Preparation characteristics of water-in-oil-water multiple emulsions using microchannel emulsification. J Colloid Inter Sci 270: 221-228

Sugiura S, Kumazawa N, Iwamoto S, Oda T, Satake M, Seki M, Nakajima M (2004b) Effect of physical properties on droplet formation in microchannel emulsification. Kagakukogaku Ronbunshu 30:129-133

Sugiura S, Oda T, Izumida Y, Aoyagi Y, Satake M, Ochiai A, Ohkohchi N, Nakajima M (2005) Size control of calcium alginate beads containing living cells using micro-nozzle array. Biomaterials 26:3327-3331

Sugiura S, Kuroiwa T, Kagota M, Nakajima M, Sato S, Mukata S, Walde P, Ichikawa S (2008) Novel method for obtaining homogeneous giant vesicles from a monodisperse water-in-oil emulsion prepared with a microfluidic device. Langmuir 24:4581- 4588

Suzuki K, Fujiki I, Hagura Y (1998) Preparation of corn oil/water and water/corn oil emulsions using PTFE membranes. Food Sci Technol 4: 164-167

Takeuchi S, Garstecki P, Weible DB, Whitesides GB (2005) An axisymmetric flow-focusing microfluidic device. Adv. Coll. Inter. 75:107-163

Tan C, Kobayashi I and Nakajima M (2005) Preparation of monodispersed

refined-bleached-deodorized (RBO) palm-olein-in-water emulsions by microchannel emulsification.

Thorsen T, Roberts EW, Arnold FH, Quske SR (2001) Dynamic pattern formation in a vesicle-generating microfluidic divice. Phys Rev Lett 86:4163- 4166

Tong J, Nakajima M, Nabetani H, Kikuchi Y (2000) Surfactant effect on production of monodispersed microspheres by microchannel method emulsification. J Surfactants Detergents 3: 285-293

Umbanhowar P B, Prasad V, Weiz DA (2000) Monodisperse emulsion generation via drop break off in a coflowing stream. Langmuir 16: 347-351

Utada AS, Lorenceau E, Link DR, Kaplan PD, Stone HA, Weitz DA (2005) Monodisperse double emulsions generated from a microfluidic device. Science 308: 537-541

van Dijke K, Kobayashi I, Schroën K, Uemura K, Nakajima M, Boom R (2010) Effect of viscosities of dispersed and continuous phases in microchannel oil-in-water emulsification. Microfluidic Nanofluidic. 9: 77-85

van Dijke K, Schroën K, Boom RM (2008) Microchannel emulsification: From computational fluid dynamics to predictive analytical model. Langumuir 24: 10107-10115

van der Zwan E, van del Sman R, Schroën K, Boom RM (2009) Lattice Boltzmann simulation of droplet formation during microchannel emulsification. J Colloid Interface Sci 335: 112-122

van der Zwan E, Schroën K, Boom R M (2009) A geometric model for the dynamics of microchannel emulsification. Langmuir 25: 7320-7327

Vladisavljević G T, Kobayashi I, Nakajima M (2006) Manufacture of monodisperse

oil-in-water emulsions at high droplet formation rates using novel asymmetric silicon microchannels. 38th Annual Meeting of the Society of Chemical Engineers, Japan, Fukuoka, pp Vb024

Vlahovska P M, Danov K D, Mehreteab A, Broze G (1997) Adsorption kinetic of ionic surfactants with detailed account for the electrostatic interactions. J Colloid Interface Sci 192: 194-206

Xu J H, Li S W, Tan J, Wang J, Luo G S (2006) Controllable preparation of monodisperse O/W and W/O emulsions in the same microfluidic device. Langmuir 22:7943-7946

Xu Q, Nakajima M (2004) The generation of highly monodisperse droplets through the breakup of hydrodinamically focused microhead in a microfluidic device. Appl Phys Lett 85: 3726-3728

Xu S, Nie Z, Seo M, Lewis P C, Kumacheva E, Garstecki P, Weible D, Gitlin I, Whitesides G M, Stone H A (2005) Generation of monodisperse particles using microfluidics: control over size, shape and composition. Angew Chemie Int Ed 44: 724-728

Yobas L, Martens S, Ong W L, Ranganathan N (2006) High performance flow-focusing geometry for spontaneous generation of monodispersed droplets. Lab Chip 6:1073-1079

ensuring my well-being in the lab.

I thank Mr. Yoshihiro Wada of EP Tech Co. Ltd. for his technical support.

My deepest gratitude is to my friends for their kind helps, for always listening to me and encourages me to succeed in my studies.

Finally, I would like to dedicate this dissertation to my family and boyfriend for their unconditional support, love, encouragement, trust and dedication to me.

May, 2015
Yanru ZHANG